Bioorganic & Medicinal Chemistry 18 (2010) 5950–5964

Contents lists available at ScienceDirect

Bioorganic & Medicinal Chemistry

journal homepage: www.elsevier.com/locate/bmc

Dual inhibitors of inosine monophosphate dehydrogenase and histone deacetylase based on a cinnamic hydroxamic acid core structure

Liqiang Chen [a,*], Riccardo Petrelli [a,d,†], Guangyao Gao [a], Daniel J. Wilson [a], Garrett T. McLean [a], Hiremagalur N. Jayaram [b], Yuk Y. Sham [a,c], Krzysztof W. Pankiewicz [a]

[a] Center for Drug Design, Academic Health Center, University of Minnesota, 516 Delaware Street S.E., Minneapolis, MN 55455, USA
[b] Department of Biochemistry and Molecular Biology, Indiana University School of Medicine and Richard Roudebush Veterans Affairs Medical Center, 1481 West Tenth Street, Indianapolis, IN 46202, USA
[c] Biomedical Informatics and Computational Biology Program, University of Minnesota, Minneapolis, MN 55455, USA
[d] School of Pharmacy, Medicinal Chemistry Unit, Università di Camerino, Via S. Agostino 1, 62032 Camerino, Italy

ARTICLE INFO

Article history:
Received 6 May 2010
Revised 19 June 2010
Accepted 23 June 2010
Available online 1 July 2010

Keywords:
Inosine monophosphate dehydrogenase
Histone deacetylase
Dual inhibitor
Cinnamic hydroxamic acid
Cancer therapy
Drug resistance

ABSTRACT

Small molecules that act on multiple biological targets have been proposed to combat the drug resistance commonly observed for cancer chemotherapy. By combining the structural features of known inhibitors of inosine monophosphate dehydrogense (IMPDH) and histone deacetylase (HDAC), dual inhibitors of IMPDH and HDAC based on the scaffold of cinnamic hydroxamic acid (CHA) have been designed, synthesized, and evaluated in biological assays. Key features, including the linker length, linker functionality, substitution position, and interacting groups, have been explored. Their individual contribution to the inhibitory activities against human IMPDH1 and IMPDH2 as well as HDAC has been assessed.

1. Introduction

Cancer cells have been characterized as those that can sustain their growth, escape growth inhibition and evade apoptosis.[1] This lack of control has been attributed to genetic mutations and functional alterations of proteins that are involved in signal transductions and cellular regulations. Extensive biological research has delineated diverse signaling pathways that regulate the processes of cell proliferation, differentiation, and apoptosis. Such information has inspired and facilitated the design of a wide range of small molecules and macromolecular biologics that target the precise mechanisms causing and driving the pathological process of a particular type of cancer. A number of targeted anticancer therapeutics have entered clinical trials and many have been approved for clinical use, greatly improving the treatment of various cancers. However, resistance to targeted therapeutics usually occurs due to gene amplification, amino acid point mutation, function redundancy and pathway cross-talking, severely reducing the efficacy of targeted therapy.[2]

The success of and challenges faced by targeted anticancer therapeutics can be exemplified by imatinib mesylate, currently a first line therapy for chronic myelogenous leukemia (CML). The hallmark of CML is Philadelphia (Ph) chromosome derived from a chromosomal translocation that fuses the genes of Bcr and Abl. The resultant Bcr-Abl tyrosine kinase is constitutively active and is expressed in 95% of CML, representing an extremely attractive target for CML therapy.[3] Imatinib inhibits this aberrant Bcr-Abl chimeric protein and interrupts the subsequent signaling cascades that eventually lead to deregulated proliferation. Imatinib has revolutionized the treatment of CML and established itself as a model for future discovery and development of targeted anticancer therapeutics. However, resistance to imatinib frequently stems from amplification of Bcr-Abl gene. More significantly, a growing number of point mutations have emerged, either interrupting imatinib's binding in the ATP binding pocket or preventing Bcr-Abl from adopting the inactive conformation to which imatinib binds.[4] The second generation of Bcr-Abl inhibitors such as nilotinib and dasatinib are able to overcome a majority of Bcr-Abl mutations. However, T315I, a critical mutation, still remains elusive.[4]

Consequently, there is an urgent need for new approaches to combat the inevitable drug resistance.[5] One strategy is to combine a targeted therapy with conventional anticancer agents or another targeted therapy. Another strategy is to design and develop a drug that simultaneously inhibits a broad spectrum of biological targets. For instance, multi-kinase inhibitors have been actively pursued for the treatment of cancers.[6] However, a broad spectrum inhibitor

* Corresponding author. Tel.: +1 612 624 2575; fax: +1 612 624 8154.
E-mail address: chenx462@umn.edu (L. Chen).
† Current address.

0968-0896/$ - see front matter © 2010 Elsevier Ltd. All rights reserved.
doi:10.1016/j.bmc.2010.06.081

usually acts on protein targets in the same family or in closely related families. As a result, cross resistance is a potential drawback.

We report herein our design, synthesis and biological evaluation of a new class of anticancer agents that inhibit both inosine monophosphate dehydrogenase (IMPDH) and histone deacetylase (HDAC). Blockage of both IMPDH and HDAC, two well-established anticancer targets with significantly different mechanisms, could reduce the probability of drug induced resistance and cross resistance.

HDAC catalyzes the deactylation of the acetyl lysine residue on histone tails. There are 18 members of human HDAC which are categorized into four classes. Class I, II, and IV HDACs require zinc metal while Class III HDACs (SIRTs) are NAD-dependent. Together with histone acetyltransferase (HAT), HDAC controls the histone acetylation level and subsequent gene expression through chromatin modification. It has been suggested that HDAC inhibitors allow the expression of certain genes that are suppressed in cancer cells.[7] In addition, a wide range of non-histone proteins have been discovered as HDAC substrates, many of which have been suggested to be important targets for cancer therapy.[8,9] Suberoylanilide hydroxamic acid (SAHA, vorinostat) (**1**, Fig. 1) and romidepsin (**7**, Fig. 1) have been approved by the Food and Drug Administration (FDA), validating HDAC inhibitors as anticancer therapeutics.

IMPDH, a nicotinamide adenine dinucleotide (NAD)-dependent enzyme,[10] catalyzes a rate-limiting step in the de novo synthesis of guanine nucleotides, which are crucial for cell growth and proliferation. There are two forms of human IMPDH, type 1 and type 2. The type 2 isoform (*h*IMPDH2) is selectively up-regulated in proliferating cells while the type 1 isoform (*h*IMPDH1) has been shown to play a key role in angiogenesis, establishing IMPDH as an attractive target for anticancer drug discovery.[11,12]

2. Results and discussion

2.1. Design

Our design of dual inhibitors was based on a premise that inhibitors targeting one enzyme can be structurally modified without compromising their initial activity while simultaneously enhancing their activity against a second target. We anticipated that key features present in individual IMPDH and HDAC inhibitors could be combined or merged into one single molecule without compromising the activity against either target. Our design was prompted by an examination of known HDAC and IMPDH inhibitors, which indicated that both groups of inhibitors exhibited considerable chemical flexibility.

Known zinc-dependent HDAC inhibitors can be divided into several classes, such as short-chain fatty acid, hydroxamic acid, benzamide, and cyclic tetrapeptide (Fig. 1).[13] A general pharmacophore, which consists of a metal binding group, linker and cap region, can be proposed for the HDAC inhibitors. For the metal binding group, a hydroxamic acid usually exhibits higher potency than the corresponding benzamide. The linker region is fairly flexible and allows for extensive structural modifications. A five to six carbon member linear side chain, such as those in SAHA (**1**, Fig. 1), fits very well in the active site of HDAC enzymes while aromatic rings such as cinnamic acid derivatives (**2**–**4**, Fig. 1) are well accommodated. The cap region tolerates a wide range of aromatic and heterocyclic aromatic group and can be exploited for possible selectivity among HDAC members.

IMPDH inhibitors can be divided into two categories based on the active sites to which they bind: IMP site and NAD site.[12] Among those targeting the NAD binding site, tiazofurin (**8**, Fig. 2) needs an initial conversion to mononucleotide and subsequent activation through the formation of an NAD analogue. Mycophenolic acid (**9**, MPA, Fig. 2) does not require activation and fits in the nicotinamide subsite of the NAD binding site. Importantly, structure-based drug design based on the MPA binding mode has yielded series of novel IMPDH inhibitors, as exemplified by VX-497 (**10**, Fig. 2), based on a *N*-[3-methoxy-4-(5-oxazolyl)phenyl]amino (MOA) moiety which was believed to bind in a fashion analogous to the substituted benzofuranone present in MPA.[14] In addition to those containing MOA, IMPDH inhibitors based on a *N*-(4-cyano-3-methoxyphenyl)amino (CMA) group have also been discovered and developed, with VX-148 (**12**, Fig. 2) as a prominent example.[15] Further explorations of structural modifications have identified additional warhead groups such as oxazolylindole,[16] cyanoindole,[17] 4-pyridylindole, isoquinoline,[18] and acridone.[19]

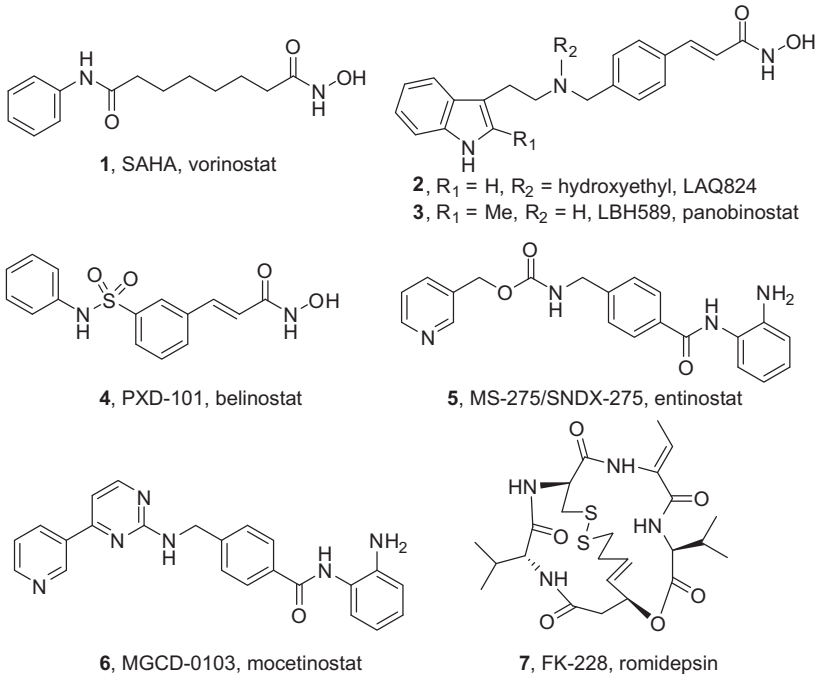

Figure 1. Examples of HDAC inhibitors.

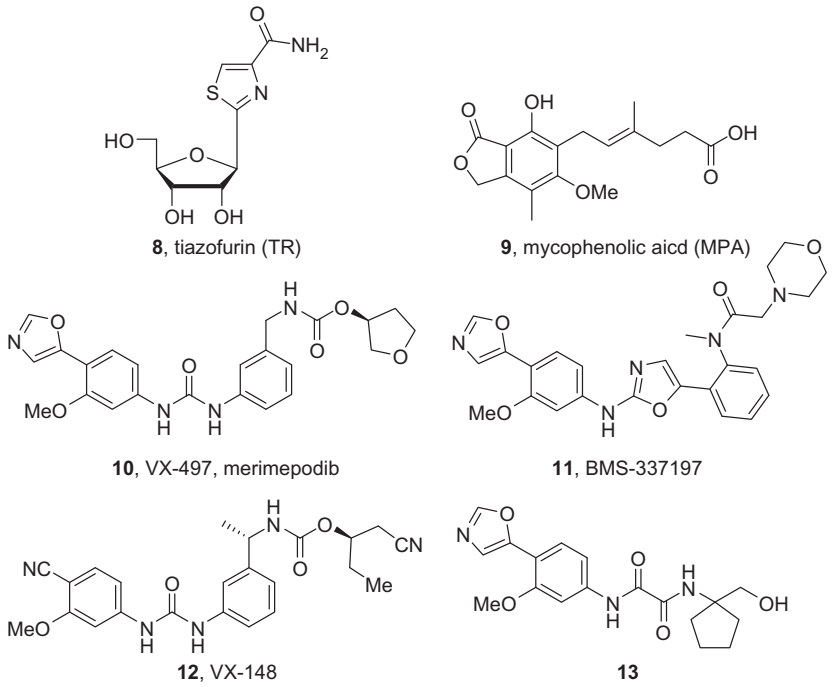

Figure 2. Examples of IMPDH inhibitors.

In addition to the warhead moiety, the linker region can also accommodate various structural modifications. VX-497, for example, contains a urea linker. Extensive structure–activity relationship (SAR) studies have revealed that the urea linker can be replaced with amide,[20] diamide[21] and guanidine linkers.[22] The warhead can also be linked through heterocycles, such as triazine,[23] oxazole,[24,25] quinolone,[26] indole,[27] quinazolinedione,[28] and quinazolinethione.[28]

Given the structural flexibility in HDAC and IMPDH inhibitors, the metal binding group such as hydroxamic acid in HDAC inhibitors and the warhead in IMPDH inhibitors can be connected via a linker that is tolerated for the inhibition of both IMPDH and HDAC. Previously we have reported our design of dual inhibitors based on either MPA or SAHA.[29] Replacement of the carboxylic acid in MPA with a hydroxamic acid led to MAHA (**14**, Fig. 3). On the other hand, substitution of the phenyl group in SAHA with 5-oxazole and methoxy groups yielded SMAHA (**15**, Fig. 3). Very recently, a similar approach has been used to generate inhibitors simultaneously targeting HDAC and tyrosine kinases.[30,31]

In our current study we devised dual inhibitors based on a cinnamic hydroxamic acid (CHA) core structure, which is present in many HDAC inhibitors (Fig. 1). The target compounds shown in Figure 4 were proposed based on a general pharmacophore model, in which a hydroxamic acid interacts with the zinc atom in the active site of HDAC. The cinnamic hydroxamic acid is connected via a linker to MOA or CMA, a warhead which is expected to bind into the NAD binding site of IMPDH. Two series of compounds (aminomethyl CHA and amino CHA series) have been conceived to evaluate the individual contribution by key structural components to the inhibitory activity of either IMPDH or HDAC. Four variations, namely the length of linker (aminomethyl vs amino), the position of substitution (*para* vs *meta*), the functionality of linker (urea vs diamide) and the nature of IMPDH-interacting groups (MOA vs CMA), are to be explored.

2.2. Chemistry

Synthesis of the aminomethyl CHA series of dual inhibitors required key aminomethyl cinnamic esters **23a** and **23b**, whose preparations are shown in Scheme 1. *para*-Substituted bromide **20a** underwent a Heck reaction to give *para*-substituted aldehyde **21a**,[32,33] which was reduced to afford alcohol **22a**. Conversion of alcohol **22a** to amine **23a** was accomplished by initial mesylation, replacement of the resultant mesylate with an azido group, and final reduction of azide to amine. Amine **23a** was isolated as a hydrochloride form. The *meta*-substituted amine **23b** was prepared from *meta*-substituted bromide **20b** in an identical sequence of reactions as depicted in Scheme 1.

para-Substituted amine **23a** and 3-methoxy-4-(5-oxazolyl)phenylamine (**24**)[20] were combined to give urea **26a** by the action of triphosgene (Scheme 2). Removal of the *tert*-butyl group was accomplished under acidic conditions to give carboxylic acid **27a**, which was in turn converted into a trityl-protected hydroxamic acid **28a** in the presence of 1-ethyl-3-(3-dimethylaminopropyl)carbodiimide hydrochloride (EDC) and 1-hydroxybenzotriazole (HOBt). Hydroxamic acid **16a** was obtained after a facile

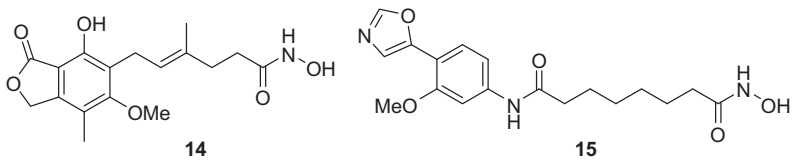

Figure 3. Dual inhibitors of IMPDH and HDAC.

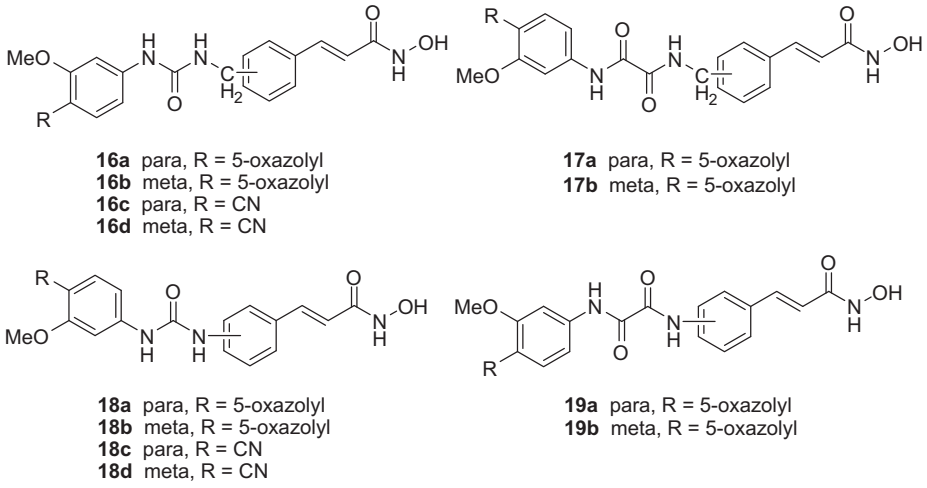

Figure 4. Dual inhibitors of IMPDH and HDAC based on CHA core structure.

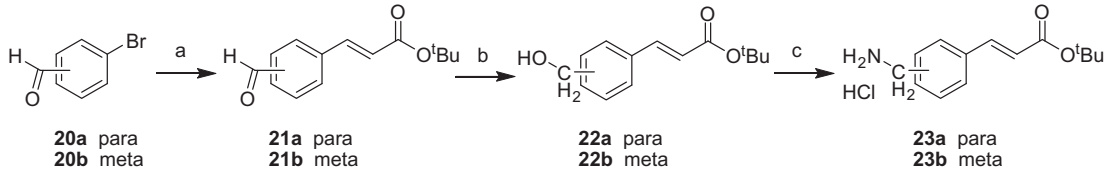

Scheme 1. Reactions and conditions: (a) *tert*-butyl acrylate, $Pd(OAc)_2$, P(*O*-tolyl)$_3$, NaOAc, DMF, 130 °C, yield 69–78%; (b) $NaBH_4$, EtOH, yield 83–86%; (c) (i) MsCl, Et_3N, THF; (ii) NaN_3, DMF; (iii) Ph_3P, THF/H_2O; (iv) HCl, diethyl ether, yield 97–98%.

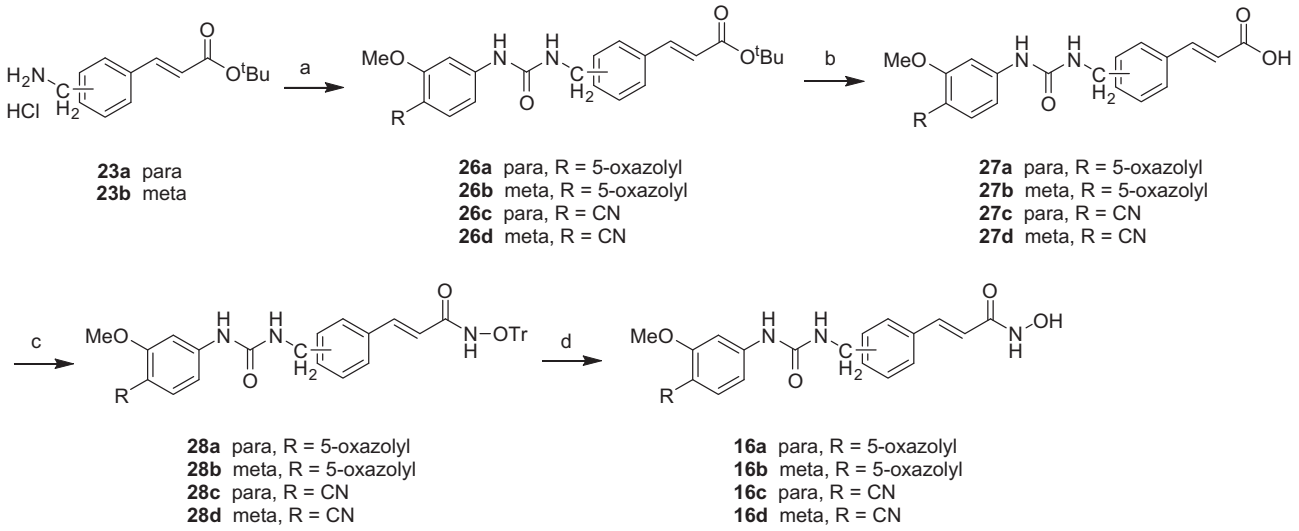

Scheme 2. Reactions and conditions: (a) aniline **24** or **25**, triphosgene, Et_3N, CH_2Cl_2, yield 26–72%; (b) TFA, CH_2Cl_2, yield 98–100%; (c) H_2N–OTr, EDC, HOBt, DMF, yield 21–62%; (d) TFA, Et_3SiH, CH_2Cl_2, yield 57–97%.

removal of the trityl protecting group. *meta*-Substituted amine **23b** and aniline **24**, after a series of chemical transformations, led to hydroxamic acid **16b**. Through similar reactions, 4-amino-2-methoxybenzonitrile (**25**)[34] was linked to amine **23a** and **23b** to give hydroxamic acids **16c** and **16d**, respectively (Scheme 2).

A coupling of *para*-substituted amine **23a** with 2-(3-methoxy-4-(oxazol-5-yl)phenylamino)-2-oxoacetic acid (**29**)[21] was mediated by benzotriazol-1-yl-oxytripyrrolidinophosphonium hexafluorophosphate (PyBOP) in the presence of *N*-methylmorpholine (NMM), giving rise to diamide **30a** (Scheme 3). Removal of the *tert*-butyl group, formation of protected hydroxamate **32a**, and cleavage of the trityl protecting group afforded diamide-linked hydroxamic acid **17a**. When *meta*-substituted amine **23b** and acid **29** were subjected to the same series of reactions, hydroxamic acid **17b** was obtained.

As shown in Scheme 4, *para*-substituted aniline **33a** and *meta*-substituted **33b** were subjected to chemical reactions similar to those depicted in Scheme 2 except for the hydrolysis reaction that was used to convert ethyl esters **34a–d** to carboxylic acids **35a–d**. Accordingly, urea-linked amino CHA compounds **18a–d** were obtained. Preparation of diamide-linked amino CHA **19a** and **19b** is depicted in Scheme 5 through transformations analogous to those

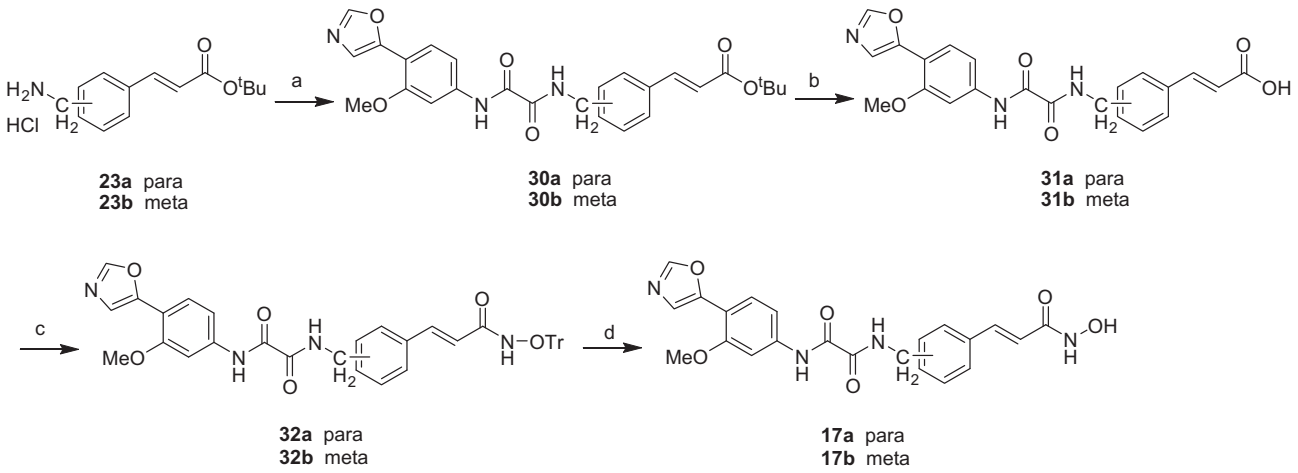

Scheme 3. Reactions and conditions: (a) compound **29**, PyBOP, NMM, DMF, yield 42%; (b) TFA, CH_2Cl_2, yield 97–100%; (c) H_2N–OTr, EDC, HOBt, DMF, yield 58–81%; (d) TFA, Et_3SiH, CH_2Cl_2, 93–94%.

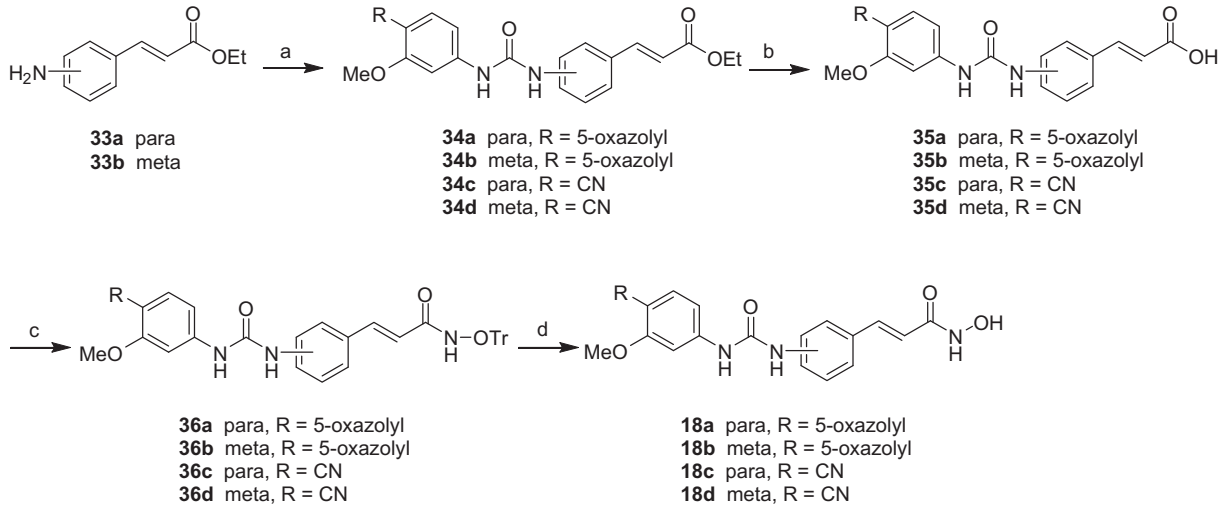

Scheme 4. Reactions and conditions: (a) aniline **24** or **25**, triphosgene, Et_3N, CH_2Cl_2, yield 27–97%; (b) NaOH, THF/H_2O/MeOH, yield 66–98%; (c) H_2N–OTr, EDC, HOBt, DMF, yield 42–54%; (d) TFA, Et_3SiH, CH_2Cl_2, yield 71–96%.

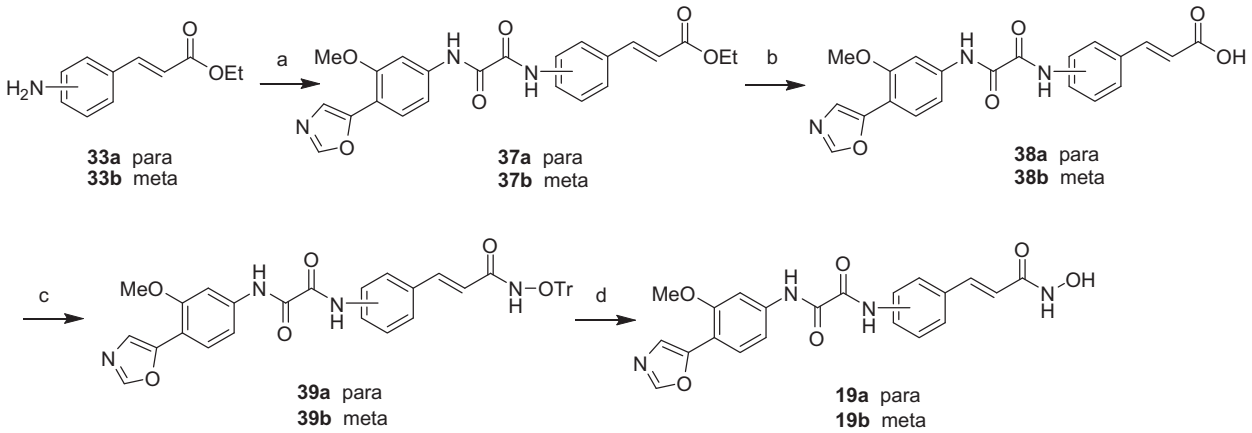

Scheme 5. Reactions and conditions: (a) compound **29**, PyBOP, NMM, DMF, yield 50–65%; (b) NaOH, THF/H_2O/MeOH, 62–77%; (c) H_2N–OTr, EDC, HOBt, DMF, yield 52–55%; (d) TFA, Et_3SiH, CH_2Cl_2, yield 22–25%.

shown in Scheme 3 except that ethyl esters **37a** and **37b** were hydrolyzed to give the corresponding acids **38a** and **38b**.

2.3. Biological evaluations

The aminomethyl CHA **16a**–**17b** and amino CHA **18a**–**19b** were tested for their activity against human IMPDH1 and IMPDH2, as well as a nuclear extract of HDAC enzymes. Compounds **16a**–**19b** were also evaluated for their anti-proliferative activity against the CML cancer cell line K562. The resulting biological data is summarized in Table 1. These dual inhibitors were weaker than VX-497 or VX-148 (Fig. 2),[15,35] generally inhibiting IMPDHs at high nanomolar to low micromolar levels. However, these compounds showed high potency against HDAC and the best compounds displayed low nanomolar activity that is comparable to that of LAQ824 (Fig. 1).[36] In order to uncover potential SAR trends, the aminometyl CHA and amino CHA series were examined individually. In each series, the influence of substitution patterns, linkers and IMPDH-interacting groups was evaluated. Furthermore, a comparison between the aminomethyl CHA and amino CHA series was also investigated.

2.3.1. Aminomethyl CHA series

In the aminomethyl CHA series **16a**–**d** and **17a**–**b**, *meta*-substituted inhibitors exhibited higher activity against IMPDH1 than the corresponding *para*-substituted compounds. A similar trend was observed against IMPDH2, even though diamide **17a** was as potent as **17b**. Inhibitors with a urea linker appeared to possess higher inhibitory activity against IMPDH1 than those with a diamide linker, as indicated by comparing ureas **16a** and **16b** with diamides **17a** and **17b**. As observed in the urea series **16a**–**d**, replacement of 5-oxazole with a cyano group greatly diminished inhibition against both IMPDH 1 and IMPDH2.

In contrast to the trend observed for the inhibition of IMPDH1 and IMPDH2, *para*-substituted ureas **16a** and **16c** displayed drastically enhanced inhibitory ability against HDAC than the corresponding *meta*-substituted ureas **16b** and **16d**. *Para*-substituted diamide **17a** was approximately threefold more potent than *meta*-substituted diamide **17b**. Urea-linked compound **16a** was more active than diamide-linked analogue **17a** whereas compounds **16b** and **17b** showed similar activity. In addition, hydroxamic acids containing a 5-oxazole displayed HDAC inhibition similar to those with a cyano group as indicated by comparing **16a** and **16b** with **16c** and **16d**.

2.3.2. Amino CHA series

In the amino CHA series **18a**–**d**, *para*-substituted ureas generally showed higher activity against both IMPDH1 and IMPDH2 than the corresponding *meta*-substituted compounds even though *para*-substituted urea **18a** was slightly less potent than *meta*-substituted urea **18b**. This trend is in contrast to the observation that *meta*-substitution generally enhanced the inhibition of human IMPDHs in the aminomethyl CHA series. Nevertheless, *para*-substituted diamide **19a** was less potent against IMPDH1 and IMPDH2 than *meta*-substituted diamide **19b**. As far as the linker is concerned, *para*-substituted urea **18a** was an IMPDH inhibitor much more active than its diamide counterpart **19a**. However, *meta*-substituted urea **18b** and *meta*-substituted diamide **19b** showed similar inhibitory activity.

Compounds containing a cyano group generally possessed weaker potency against either IMPDH1 or IMPDH2 than their 5-oxazole counterparts. For example, *para*-substituted urea **18a** and **18b** showed significantly higher activity against IMPDH1 than **18c** and **18d**. A similar enhancement of activity was also observed for compound **18b** against IMPDH2 in relation to compound **18d**. However, 5-oxazole-containing compound **18a** exhibited inhibition of IMPDH2 that was nearly identical to that of compound **18c**.

Mirroring the trend observed for the urea-linked aminomethyl CHA series, the urea-linked *para*-substituted compounds were significantly more potent inhibitors of HDAC than the corresponding *meta*-substituted counterparts, regardless of whether MOA or CMA was incorporated. However, the trend was reversed for diamide-linked compounds as HDAC inhibitors, in which *meta*-substituted **19b** is nearly 10-fold more potent than *para*-substituted **19a**. This observation indicates that a *meta*-substitution seems to favor HDAC inhibition for the diamide-linked compounds, contradicting the observation for the urea-linked compounds.

When the linker is considered, diamide-linked compounds such as **19a** and **19b** were weaker HDAC inhibitors than those with urea-linked compounds **18a** and **18b**, a trend consistent with that observed in the aminomethyl CHA series. Compounds with CMA were as potent inhibitors as those with MOA, a phenomenon that was also observed in the aminomethyl CHA series.

Table 1
Biological evaluations of dual inhibitors of IMPDH and HDAC

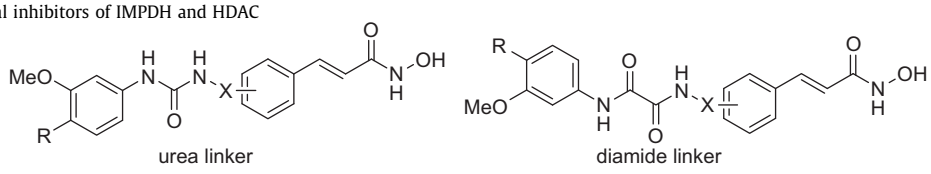

Compound	X	Position	Linker	R	IMPDH1 K_i^{app} (μM)	IMPDH2 K_i^{app} (μM)	HDAC nuclear extract IC_{50} (μM)	K562 cell proliferation 50 (μM)
16a	CH_2	*para*	Urea	5-Oxazolyl	7.8 ± 0.8	1.2 ± 0.2	0.026 ± 0.006	3.5
16b	CH_2	*meta*	Urea	5-Oxazolyl	2.3 ± 0.1	0.34 ± 0.06	0.83 ± 0.39	18
16c	CH_2	*para*	Urea	CN	>100	11 ± 1	0.036 ± 0.020	ND[a]
16d	CH_2	*meta*	Urea	CN	44 ± 18	2.6 ± 0.3	0.64 ± 0.56	28
17a	CH_2	*para*	Diamide	5-Oxazolyl	17 ± 10	1.4 ± 0.6	0.23 ± 0.10	5.3
17b	CH_2	*meta*	Diamide	5-Oxazolyl	4.4 ± 0.5	1.5 ± 0.1	0.89 ± 0.28	>100
18a	None	*para*	Urea	5-Oxazolyl	0.30 ± 0.05	0.25 ± 0.12	0.55 ± 0.14	4.9
18b	None	*meta*	Urea	5-Oxazolyl	0.58 ± 0.06	0.12 ± 0.01	3.0 ± 0.7	>100
18c	None	*para*	Urea	CN	1.2 ± 0.3	0.23 ± 0.10	0.63 ± 0.46	4.0
18d	None	*meta*	Urea	CN	8.2	1.2	3.4 ± 0.7	38
19a	None	*para*	Diamide	5-Oxazolyl	7.1 ± 0.6	1.8 ± 0.3	17 ± 12	72
19b	None	*meta*	Diamide	5-Oxazolyl	0.46 ± 0.03	0.20 ± 0.02	1.8 ± 0.5	28

[a] ND, not determined due to low aqueous solubility.

2.3.3. Aminomethyl CHA series versus amino CHA series

When the aminomethyl CHA and amino CHA series were compared, it was clear that compounds included in the amino CHA series exhibited higher potency against human IMPDH1 and IMPDH2 with the exception of compound **19a**, which displayed approximately the same potency against IMPDH2 as its aminomethyl counterpart compound **17a**. However, when the inhibition of HDAC was under consideration, aminomethyl CHA series consistently showed higher activity than the corresponding the amino CHA series.

From our SAR studies as discussed above, it can be concluded that in the aminomethyl series a *meta*-substitution pattern is generally preferred for the inhibition of IMPDHs whereas a *para*-substitution leads to potent inhibition of HDAC enzymes. In other words, structural modifications which increased the inhibitory activity towards IMPDH decreased that against HDAC. Compounds in the aminomethyl series generally inhibited human IMPDHs at micromolar levels whereas they possessed anti-HDAC activity at sub-micromolar levels. Worth noting are compounds **16a** and **16c**, which displayed anti-HDAC IC_{50}'s of approximately 30 nM.

In the amino CHA series, the SAR trend observed for compounds connected via a urea linker contradicts that drawn from compounds with a diamide linker. A *meta*-substitution is necessary for increased potency for compounds with a diamide linker. In contrast, in the urea-linked compounds, a *para*-substitution is generally preferred for higher activity against both human IMPDH and HDAC. These convergent SAR trends allowed for simultaneous enhancement of activity against IMPDH and HDAC, a task which was not feasible in the aminomethyl CHA series. Several compounds in the amino CHA series, such as compound **18a** and **18c**, exhibited potent and comparable activity against IMPDH and HDAC.

2.3.4. Anti-proliferation assay in K562 cells

Compounds **16a**–**19b** showed modest to weak inhibition of K562 as indicated by IC_{50}'s above micromolar levels. The IC_{50}'s did not appear to correlate with compounds' ability to inhibit either IMPDH or HDAC. The low inhibitory activity and erratic SAR trend might be attributed to the poor aqueous solubility of these compounds, a phenomenon that was observed in our synthetic efforts.

2.4. Computational modeling

A HDAC1 homology model was constructed based on the solved X-ray crystallographic structure of histone deacetylase-like protein (HDLP) in complex with SAHA.[37] The initial sequence alignment of HDAC1-11 and HDLP showed HDLP has the highest sequence similarity to HDAC1 with 59% sequence identity in the catalytic site. Compound **16a**, which is the most potent HDAC inhibitor in the current series of dual inhibitor, and SAHA were docked into the HDAC1 homology model (Fig. 5). Compound **16a**, with a *para*-substitution pattern on the cinnamic ring, fits snugly into the narrow tube-like catalytic cavity in a manner similar to SAHA, a prototype of HDAC inhibitors. For both compounds, the hydroxamic acid, along with residues Asp264, His178, and Asp176, coordinates with the zinc ion at the bottom of the cavity, accounting for a significant fraction of the total energy contributions. Additionally, for compound **16a** the phenyl ring of CHA is involved in π–π stacking with Phe150 and Phe205. The MOA moiety binds in the cap region in a fashion very similar to that of SAHA, engaging in a favorable interaction with Pro29. Judged by the binding mode of compound **16a** in HDAC1, a *para*-substitution is clearly preferred in order to fit in the tube-like catalytic cavity whereas a *meta*-substitution pattern elicits an unfavorable clash with the residues that form the wall. Therefore, it is no surprise that compounds with a *para*-substitution were consistently more potent than ones that are *meta*-substituted. Since the MOA or CMA binds outside the cavity and is engaged in similar interactions, compounds with MOA displayed virtually identical activity against HDAC when compared to similar compounds with CMA.

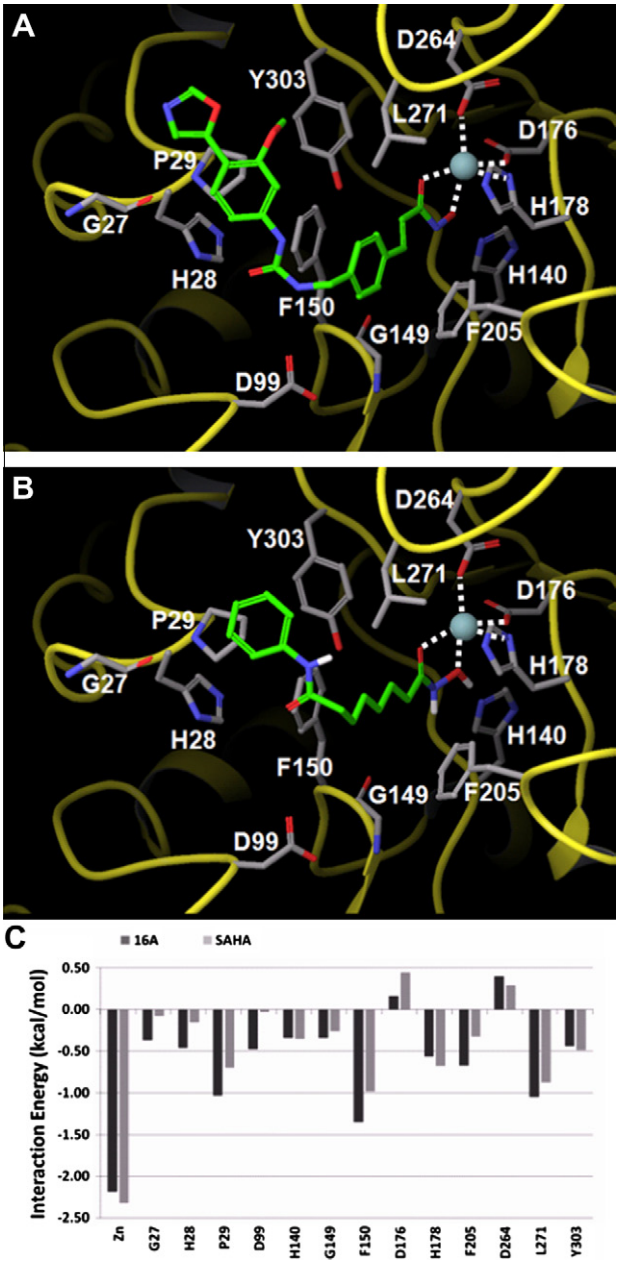

Figure 5. Comparison between compound **16a** (A) and SAHA (B) within HDAC1 homology model binding site. All key amino acid residues are shown. (C) Per residue interaction energy in kcal/mol of compound **16a** (A) and SAHA (B) within the HDAC1 binding site.

Modeling of compounds **18a** and **18b** into the NAD binding pocket of the solved X-ray crystallographic structure of *h*IMPDH2 was based on the binding mode of VX-497 (Fig. 6) as previously reported.[14] Both compounds engage in an energetically favorable stacking interaction with IMP, the enzymatic reaction substrate. The urea functionality forms hydrogen bonds with Asp274, a key interaction observed for VX-497 and its analogues. For compound **18a** with its *para*-substitution on the cinnamic phenyl moiety, the hydroxamic acid side chain is extended into the adenosine subsite of the NAD binding site. For compound **18b**, the hydroxamic

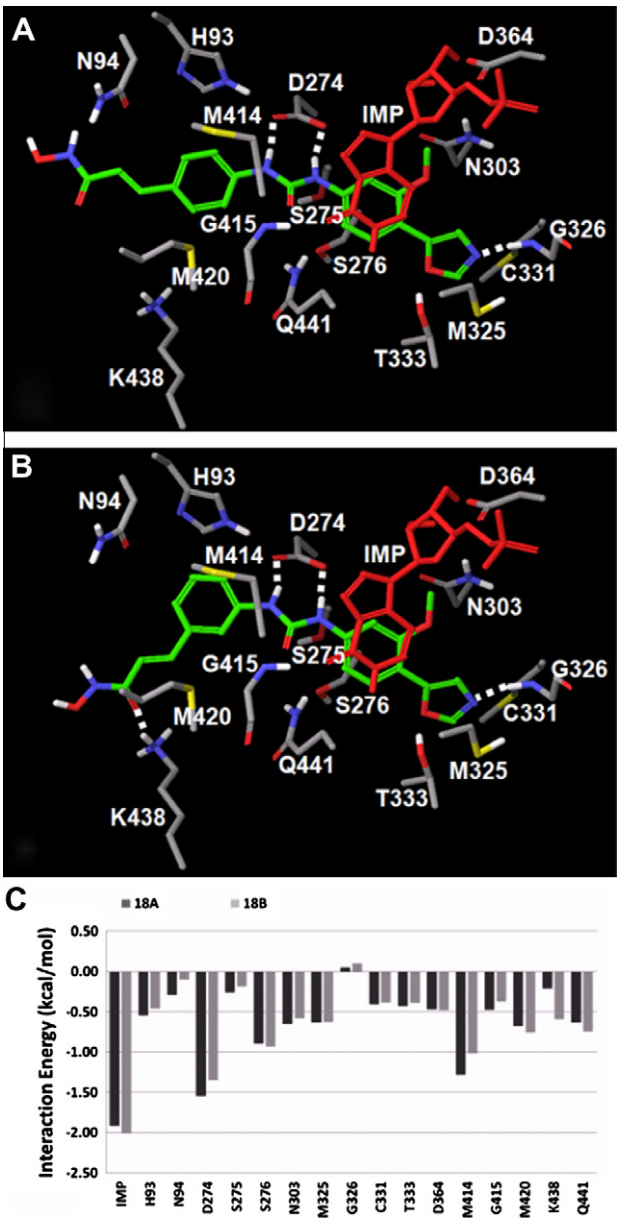

Figure 6. Comparison between compound **18a** (A) and **18b** (B) within Human IMPDH Type II binding site. All key amino acid residues are shown. (C) Per residue interaction energy in kcal/mol of compound **18a** and **18b** within the *h*IMPDH2 NAD binding site.

acid is projected into a channel that is perpendicular to the NAD binding site, emulating the bind mode of VX-497. The comparison between compounds **18a** and **18b** indicates that either substitution pattern is tolerated and does not significantly alter a compound's ability to inhibit IMPDH, at least in the urea series.

Our molecular modeling and SAR study clearly suggest a general approach for the design of compounds with balanced activities against both IMPDH and HDAC. In these compounds a desired *para*-substitution pattern would confer an extended and linear molecular shape like that of compound **18a**, a structural feature accommodated by HDAC as well as IMPDH.

3. Conclusions

By combining structural features from known inhibitors of IMPDH and HDAC, we have been able to design, synthesize and evaluate a new type of dual inhibitors of IMPDH and HDAC based on a CHA core structure. Two series of compounds, namely the aminomethyl CHA and amino CHA series, have been conceived. Variations of key components in either series allowed us to assess the individual contribution of these elements. In the aminomethyl CHA series, a *meta*-substitution pattern is desired for improved inhibition of IMPDHs whereas a *para*-substitution is generally preferred for inhibition of IMPDH in the urea-linked amino CHA compounds. Nevertheless, a *para*-substitution pattern leads to higher activity against HDAC in both series except for diamide-linked amino CHA compounds. While the SAR trends for the enhancement of IMPDH and HDAC inhibition are divergent in the aminomethyl CHA series, the convergent SAR observed in the amino CHA series has permitted us to prepare compounds with comparable activity against both IMPDH and HDAC. In summary, we have successfully designed CHA-based dual inhibitors of IMPDH and HDAC by exploiting structural flexibility, a strategy which can be applied to devise new classes of dual inhibitors. Our SAR study and molecular modeling have also revealed a general approach for the design of balanced dual inhibitors. All these inhibitors may prove valuable to combat the inevitable drug resistance emerging from targeted cancer chemotherapies.

4. Experimental

4.1. General methods

All commercial reagents (Sigma–Aldrich, Acros) were used as provided unless otherwise indicated. An anhydrous solvent dispensing system (J. C. Meyer) using two packed columns of neutral alumina was used for drying THF, Et_2O, and CH_2Cl_2, while two packed columns of molecular sieves were used to dry DMF. Solvents were dispensed under argon. Flash chromatography was performed with Ultra Pure silica gel (Silicycle) with the indicated solvent system. Melting points were determined on a Mel-Temp apparatus and were uncorrected. Nuclear magnetic resonance spectra were recorded on a Varian 600 MHz with Me_4Si or signals from residual solvent as the internal standard for ^1H or ^{13}C. Chemical shifts are reported in ppm, and signals are described as s (singlet), d (doublet), t (triplet), q (quartet), m (multiplet), bs (broad singlet), and dd (double doublet). Values given for coupling constants are first order. High resolution mass spectra were recorded on an Agilent TOF II TOF/MS instrument equipped with either an ESI or APCI interface.

4.2. Chemical synthesis

4.2.1. (*E*)-*tert*-Butyl 3-(4-formylphenyl)acrylate (21a)

A solution of 4-bromobenzaldehyde (**20a**, 9.33 g, 50.4 mmol), *tert*-butyl acrylate (10.9 mL, 75.1 mmol), $Pd(OAc)_2$ (226 mg, 1.01 mmol), P(*O*-tolyl)$_3$ (928 mg, 3.05 mmol), and NaOAc (8.49 g, 103 mmol) in dry DMF (100 mL) in a sealed flask was evacuated and then back-filled with argon five times. The mixture was heated at 130 °C for 24 h. After cooling to rt, the mixture was filtered through a pad of Celite and washed with EtOAc. After the filtrate was concentrated, the residue was dissolved in EtOAc (500 mL) and washed with water (2 × 200 mL) and brine (2 × 200 mL). The organic layer was dried over Na_2SO_4 and filtered. The filtrate was concentrated and the residue was triturated with hot hexanes (100 mL). After filtration, aldehyde **21a** was obtained as a white solid (8.08 g, 69%). ^1H NMR ($CDCl_3$, 600 MHz) δ 10.02 (s, 1H), 7.89 (d, J = 7.8 Hz, 2H), 7.66 (d, J = 7.8 Hz, 2H), 7.61 (d, J = 16.2 Hz, 1H), 6.48 (d, J = 16.2 Hz, 1H), 1.54 (s, 9H). HRMS calcd for $C_{14}H_{17}O_3$ 233.1178 $(M+H)^+$, found 233.1179.

4.2.2. (*E*)-*tert*-Butyl 3-(3-formylphenyl)acrylate (21b)

Following procedures similar to those described for aldehyde **21a**, 3-bromobenzaldehyde (**20b**, 5.90 mL, 50.4 mmol) was converted into aldehyde **21b** as yellowish syrup (9.17 g, 78%). ^{1}H NMR ($CDCl_3$, 600 MHz) δ 10.01 (s, 1H), 7.98 (s, 1H), 7.84 (d, J = 7.8 Hz, 1H), 7.72 (d, J = 7.8 Hz, 1H), 7.60 (d, J = 16.2 Hz, 1H), 7.53 (d, J = 7.5 Hz, 1H), 6.44 (d, J = 16.2 Hz, 1H), 1.51 (s, 9H). HRMS calcd for $C_{14}H_{17}O_3$ 233.1178 $(M+H)^+$, found 233.1185.

4.2.3. (*E*)-*tert*-Butyl 3-(4-(hydroxymethyl)phenyl)acrylate (22a)

To a solution of aldehyde **21a** (3.66 g, 15.8 mmol) in EtOH (100 mL) was added $NaBH_4$ (2.38 g, 62.9 mmol) in portions within 30 min. The resulting mixture was allowed to stir at rt for 1 h and concentrated. The residue was dissolved in water (100 mL) and acidified to pH $\approx$ 5. The solid formed was filtered, washed with water and then dried to give alcohol **22a** as a white solid (3.05 g, 83%). ^{1}H NMR ($CDCl_3$, 600 MHz) δ 7.54 (d, J = 16.2 Hz, 1H), 7.47 (d, J = 6.0 Hz, 2H), 7.34 (d, J = 6.0 Hz, 2H), 6.33 (d, J = 15.6 Hz, 1H), 4.68 (s, 2H), 1.81 (br s, 1H), 1.54 (s, 9H). HRMS calcd for $C_{14}H_{19}O_3$ 235.1334 $(M+H)^+$, found 235.1329.

4.2.4. (*E*)-*tert*-Butyl 3-(3-(hydroxymethyl)phenyl)acrylate (22b)

Following procedures similar to those described for alcohol **22a**, aldehyde **21b** (4.83 g, 20.8 mmol) was reduced with $NaBH_4$ (3.14 g, 83.0 mmol) to give alcohol **22b** as a yellowish syrup (4.20 g, 86%). ^{1}H NMR ($CDCl_3$, 600 MHz) δ 7.54 (d, J = 15.6 Hz, 1H), 7.48 (s, 1H), 7.39 (t, J = 4.2 Hz, 1H), 7.34–7.30 (m, 2H), 6.34 (d, J = 16.2 Hz, 1H), 4.68 (s, 2H), 1.50 (s, 9H). HRMS calcd for $C_{14}H_{19}O_3$ 235.1334 $(M+H)^+$, found 235.1337.

4.2.5. (*E*)-*tert*-Butyl 3-(4-(aminomethyl)phenyl)acrylate hydrochloride (23a)

To a solution of alcohol **22a** (2.98 g, 12.7 mmol) and Et_3N (3.60 mL, 25.8 mmol) in anhydrous THF (80 mL) at 0 °C was added dropwise MsCl (1.50 mL, 19.3 mmol). The mixture was allowed to stir at 0 °C for 1 h, warm to rt and stir at rt for 1 h. After the reaction mixture was diluted with EtOAc (400 mL), the resulting solution was washed with water (100 mL), satd $NaHCO_3$ (100 mL), water (100 mL) and brine (200 mL). The organic layer was dried over Na_2SO_4 and filtered. The filtrate was concentrated and re-dissolved in anhydrous DMF (60 mL). After NaN_3 (1.84 g, 28.3 mmol) was added at rt, the resulting mixture was heated at 50 °C for 30 min and cooled to rt. The mixture was then diluted with EtOAc (300 mL) and washed with water (3 $\times$ 60 mL) and brine (2 $\times$ 100 mL). The organic layer was dried over Na_2SO_4 and filtered. The filtrate was concentrated and re-dissolved in a mixture of THF (60 mL) and water (6 mL). After PPh_3 (4.34 g, 16.6 mmol) was added at rt, the reaction mixture was allowed to stir at rt overnight and then concentrated. The residue was dissolved in Et_2O (15 mL), and hexanes (200 mL) was added. The solid precipitated was filtered and washed with Et_2O/hexanes. The filtrate was concentrated and the residue was dissolved in hexanes (600 mL). After an addition of a solution of HCl in Et_2O (1.0 M, 30 mL), the solid precipitated was filtered, washed and dried to give amine hydrochloride **23a** as a white solid (3.37 g, 98%). ^{1}H NMR (CD_3OD, 600 MHz) δ 7.66 (d, J = 8.4 Hz, 2H), 7.59 (d, J = 16.2 Hz, 1H), 7.51 (d, J = 8.4 Hz, 2H), 6.48 (d, J = 16.2 Hz, 1H), 4.15 (s, 2H), 1.53 (s, 9H). HRMS calcd for $C_{14}H_{20}NO_2$ 234.1488 $(M+H)^+$, found 234.1495.

4.2.6. (*E*)-*tert*-Butyl 3-(3-(aminomethyl)phenyl)acrylate hydrochloride (23b)

Following procedures similar to those described for amine **23a**, alcohol **22b** (3.86 g, 16.5 mmol) was converted into amine hydrochloride **23b** as a white solid (4.33 g, 97%). ^{1}H NMR (CD_3OD, 600 MHz) δ 7.71 (s, 1H), 7.60 (d, J = 16.2 Hz, 1H), 7.56 (td, J = 7.5, 3.0 Hz, 1H), 7.53–7.47 (m, 2H), 6.52 (d, J = 16.2 Hz, 1H), 4.16 (s, 2H), 1.53 (s, 9H). HRMS calcd for $C_{14}H_{20}NO_2$ 234.1488 $(M+H)^+$, found 234.1506.

4.2.7. *tert*-Butyl ester 26a

To a solution of 3-methoxy-4-(oxazol-5-yl)aniline[20] (456 mg, 2.40 mmol) in dry CH_2Cl_2 (25 mL) were added triphosgene (242 mg, 0.82 mmol) and Et_3N (0.34 mL, 2.44 mmol). The resulting mixture was heated at reflux for 1 h. After cooling to rt, additional Et_3N (1.0 mL, 7.2 mmol) was added, followed by an addition of (*E*)-*tert*-butyl 3-(4-(aminomethyl)phenyl)acrylate hydrochloride (777 mg, 2.88 mmol). The mixture was allowed to stir at rt for 24 h and then concentrated. The residue was dissolved in MeOH (15 mL) and slowly added to ice/water (150 mL plus 20 mL of 1 N HCl). The solid precipitate was washed with water, collected and purified by silica gel column chromatography to give *tert*-butyl ester **26a** as a light-yellow solid (414 mg, 38%). ^{1}H NMR (CD_3OD, 600 MHz) δ 8.14 (s, 1H), 7.62 (d, J = 9.0 Hz, 1H), 7.58–7.52 (m, 3H), 7.44 (d, J = 1.8 Hz, 1H), 7.40–7.35 (m, 3H), 6.92 (dd, J = 8.2, 1.8 Hz, 1H), 6.40 (d, J = 15.6 Hz, 1H), 4.42 (s, 2H), 3.92 (s, 3H), 1.52 (s, 9H). HRMS calcd for $C_{25}H_{27}N_3O_5Na$ 472.1842 $(M+Na)^+$, found 472.1810.

4.2.8. *tert*-Butyl ester 26b

Following procedures similar to those described for *tert*-butyl ester **26a**, (*E*)-*tert*-butyl 3-(3-(aminomethyl)phenyl)acrylate hydrochloride (776 mg, 2.88 mmol) was converted into *tert*-butyl ester **26b** as a light-yellow solid (284 mg, 26%). ^{1}H NMR (CD_3OD, 600 MHz) δ 8.14 (s, 1H), 7.62 (d, J = 8.4 Hz, 1H), 7.57 (d, J = 16.2 Hz, 1H), 7.55 (s, 1H), 7.49–7.45 (m, 1H), 7.44 (d, J = 1.8 Hz, 1H), 7.40–7.36 (m, 3H), 6.92 (dd, J = 8.1, 2.1 Hz, 1H), 6.44 (d, J = 15.6 Hz, 1H), 4.42 (s, 2H), 3.94 (s, 3H), 1.52 (s, 9H). HRMS calcd for $C_{25}H_{27}N_3O_5Na$ 472.1842 $(M+Na)^+$, found 472.1802.

4.2.9. *tert*-Butyl ester 26c

Following procedures similar to those described for *tert*-butyl ester **26a**, (*E*)-*tert*-butyl 3-(4-(aminomethyl)phenyl)acrylate hydrochloride (**23a**, 850 mg, 3.15 mmol) and 4-amino-2-methoxybenzonitrile[34] (**25**, 443 mg, 2.40 mmol) were coupled to give *tert*-butyl ester **26c** as a yellowish solid (705 mg, yield 72%). ^{1}H NMR ($CDCl_3$, 600 MHz) δ 7.76 (s, 1H), 7.59 (s, 1H), 7.45 (d, J = 15.6 Hz, 1H), 7.34–7.30 (m, 3H), 7.28–7.24 (m, 2H), 6.63 (dd, J = 8.4, 1.2 Hz, 1H), 6.24 (d, J = 16.2 Hz, 1H), 5.86 (t, J = 5.7 Hz, 1H), 4.43 (d, J = 5.4 Hz, 2H), 3.84 (s, 3H), 1.54 (s, 9H). HRMS calcd for $C_{23}H_{26}N_3O_4$ 408.1923 $(M+H)^+$, found 408.1915.

4.2.10. *tert*-Butyl ester 26d

Following procedures similar to those described for *tert*-butyl ester **26a**, (*E*)-*tert*-butyl 3-(3-(aminomethyl)phenyl)acrylate hydrochloride (**23b**, 850 mg, 3.15 mmol) and 4-amino-2-methoxybenzonitrile (**25**, 443 mg, 2.40 mmol) were coupled to give *tert*-butyl ester **26d** as an off-white solid (623 mg, yield 64%) ^{1}H NMR ($CDCl_3$, 600 MHz) δ 7.64 (s, 1H), 7.57 (d, J = 1.2 Hz, 1H),7.46 (d, J = 16.2 Hz, 1H), 7.36–7.24 (m, 6H), 6.62 (dd, J = 9.0, 1.2 Hz, 1H), 6.30 (d, J = 15.6 Hz, 1H), 5.77 (t, J = 5.7 Hz, 1H), 4.40 (d, J = 6.0 Hz, 2H), 3.84 (s, 3H), 1.52 (s, 9H). HRMS calcd for $C_{23}H_{25}N_3O_4Na$ 430.1737 $(M+Na)^+$, found 430.1715.

4.2.11. Carboxylic acid 27a

A solution of *tert*-butyl ester **26a** in dry CH_2Cl_2 (6 mL) and TFA (6 mL) was allowed to stir at rt overnight and then concentrated. After co-evaporation with toluene, carboxylic acid **27a** was obtained as a light-yellow solid (292 mg, 99%). ^{1}H NMR (DMSO-d_6, 600 MHz) δ 8.92 (s, 1H), 8.32 (s, 1H), 7.67–7.58 (m, 3H), 7.56 (d, J = 16.2 Hz, 1H), 7.53 (d, J = 8.4 Hz, 1H), 7.43 (s, 1H), 7.36 (s, 1H), 7.33 (d, J = 7.8 Hz, 2H), 7.01 (d, J = 7.8 Hz, 1H), 6.82 (t, J = 5.7 Hz, 1H), 6.49 (d, J = 15.6 Hz, 1H), 4.33 (d, J = 6.0 Hz, 2H), 3.87 (s, 3H). HRMS calcd for $C_{21}H_{20}N_3O_5$ 394.1397 $(M+H)^+$, found 394.1415.

4.2.12. Carboxylic acid 27b

Following procedures similar to those described for carboxylic acid **27a**, *tert*-butyl ester **26b** (257 mg, 0.57 mmol) was converted into carboxylic acid **27b** as a light-yellow solid (226 mg, 100%). ^{1}H NMR (DMSO-d_6, 600 MHz) δ 8.89 (s, 1H), 8.31 (s, 1H), 7.62–7.58 (m, 2H), 7.57–7.51 (m, 3H), 7.43 (s, 1H), 7.40–7.33 (m, 3H), 7.01 (dd, J = 8.4, 1.8 Hz, 1H), 6.80 (t, J = 5.7 Hz, 1H), 6.50 (d, J = 15.6 Hz, 1H), 4.33 (d, J = 5.4 Hz, 2H), 3.87 (s, 3H). HRMS calcd for $C_{21}H_{20}N_3O_5$ 394.1397 $(M+H)^+$, found 394.1413.

4.2.13. Carboxylic acid 27c

Following procedures similar to those described for carboxylic acid **27a**, *tert*-butyl ester **26c** (658 mg, 1.62 mmol) was converted into carboxylic acid **27c** as a pale solid (570 mg, 100%). ^{1}H NMR (DMSO-d_6, 600 MHz) δ 12.36 (br s, 1H), 9.25 (s, 1H), 7.64 (d, J = 8.4 Hz, 2H), 7.56 (d, J = 15.6 Hz, 1H), 7.51 (d, J = 9.0 Hz, 1H), 7.46 (d, J = 1.2 Hz, 1H), 7.32 (d, J = 7.8 Hz, 2H), 7.02–6.94 (m, 2H), 6.49 (d, J = 15.6 Hz, 1H), 4.32 (d, J = 6.0 Hz, 2H), 3.83 (s, 3H). HRMS calcd for $C_{19}H_{18}N_3O_4$ 352.1291 $(M+H)^+$, found 352.1285.

4.2.14. Carboxylic acid 27d

Following procedures similar to those described for carboxylic acid **27a**, *tert*-butyl ester **26d** (567 mg, 1.39 mmol) was converted into carboxylic acid **27d** as a pale solid (480 mg, 98%). ^{1}H NMR (DMSO-d_6, 600 MHz) δ 9.21 (s, 1H), 7.59 (d, J = 6.0 Hz, 1H), 7.55 (d, J = 5.4 Hz, 1H), 7.51 (d, J = 9.0 Hz, 1H), 7.46 (s, 1H), 7.38 (t, J = 7.5 Hz, 1H), 7.34 (d, J = 7.2 Hz, 1H), 6.98 (dd, J = 9.0, 1.2 Hz, 1H), 6.94 (t, J = 5.7 Hz, 1H), 6.50 (d, J = 16.2 Hz, 1H), 4.32 (d, J = 5.4 Hz, 2H), 3.83 (s, 3H). HRMS calcd for $C_{19}H_{18}N_3O_4$ 352.1291 $(M+H)^+$, found 352.1280.

4.2.15. Protected hydroxamate 28a

A solution of carboxylic acid **27a** (272 mg, 0.69 mmol), 1-ethyl-3-3(3-dimethylaminopropyl)carbodiimide hydrochloride (EDC, 410 mg, 2.07 mmol), 1-hydroxy-benzotriazole (HOBt, 189 mg, 1.40 mmol) and *O*-tritylhydroxylamine (380 mg, 1.38 mmol) in anhydrous DMF (10 mL) was stirred at rt for 4 d. After concentration, the residue was diluted with EtOAc (60 mL) and washed with water (10 mL), satd $NaHCO_3$ (10 mL), water (10 mL) and brine (30 mL). The organic layer was dried over Na_2SO_4 and filtered. The filtrate was concentrated and the residue was purified by silica gel column chromatography (0–4% MeOH/CH_2Cl_2) to give protected hydroxamate **28a** as a yellowish solid (281 mg, 62%). ^{1}H NMR (DMSO-d_6, 600 MHz) δ 10.37 (s, 1H), 8.84 (s, 1H), 8.32 (s, 1H), 7.53 (d, J = 8.4 Hz, 1H), 7.48–7.40 (m, 3H), 7.40–7.18 (m, 18H), 7.00 (d, J = 8.4 Hz, 1H), 6.71 (t, J = 5.7 Hz, 1H), 6.44 (d, J = 16.2 Hz, 1H), 4.29 (d, J = 5.4 Hz, 2H), 3.86 (s, 3H). HRMS calcd for $C_{40}H_{34}N_4O_5Na$ 673.2421 $(M+Na)^+$, found 673.2421.

4.2.16. Protected hydroxamate 28b

Following procedures similar to those described for protected hydroxamate **28a**, carboxylic acid **27b** (206 mg, 0.52 mmol) was converted into protected hydroxamate **28b** as a yellowish solid (71 mg, 21%). ^{1}H NMR (DMSO-d_6, 600 MHz) δ 10.42 (s, 1H), 8.81 (s, 1H), 8.32 (s, 1H), 7.53 (d, J = 8.4 Hz, 1H), 7.44–7.18 (m, 21H), 7.00 (d, J = 8.4 Hz, 1H), 6.71 (t, J = 5.7 Hz, 1H), 6.47 (d, J = 15.6 Hz, 1H), 4.29 (d, J = 6.0 Hz, 2H), 3.86 (s, 3H). HRMS calcd for $C_{40}H_{34}N_4O_5Na$ 673.2421 $(M+Na)^+$, found 673.2422.

4.2.17. Protected hydroxamate 28c

Following procedures similar to those described for protected hydroxamate **28a**, carboxylic acid **27c** (538 mg, 1.53 mmol) was converted into protected hydroxamate **28c** as a pale solid (505 mg, 54%). ^{1}H NMR (DMSO-d_6, 600 MHz) δ 10.39 (s, 1H), 9.20 (s, 1H), 7.56–7.16 (m, 21H), 6.98 (d, J = 6.0 Hz, 1H), 6.89 (s, 1H), 6.45 (d, J = 14.4 Hz, 1H), 4.29 (s, 2H), 3.82 (s, 3H). HRMS calcd for $C_{38}H_{31}N_4O_4$ 607.2345 $(M-H)^-$, found 607.2340.

4.2.18. Protected hydroxamate 28d

Following procedures similar to those described for protected hydroxamate **28a**, carboxylic acid **27b** (459 mg, 1.31 mmol) was converted into protected hydroxamate **28d** as a pale solid (491 mg, 62%). ^{1}H NMR (DMSO-d_6, 600 MHz) δ 10.44 (s, 1H), 9.16 (s, 1H), 7.51 (d, J = 8.4 Hz, 1H), 7.45 (s, 1H), 7.42–7.18 (m, 20H), 6.97 (d, J = 6.6 Hz, 1H), 6.88 (s, 1H), 6.48 (d, J = 15.6 Hz, 1H), 4.28 (d, J = 4.8 Hz, 2H), 3.82 (s, 3H). HRMS calcd for $C_{38}H_{31}N_4O_4$ 607.2345 $(M-H)^-$, found 607.2341.

4.2.19. Hydroxamic acid 16a

To a suspension of protected hydroxamate **28a** (256 mg, 0.39 mmol) in anhydrous CH_2Cl_2 (10 mL) was added TFA (0.50 mL). The resulting yellow solution was treated with Et_3SiH till there was no change of color. After stirring for additional 40 min, the solid precipitate was filtered, washed with CH_2Cl_2 and collected to give hydroxamic acid **16a** as a yellowish solid (151 mg, 94%). ^{1}H NMR (DMSO-d_6, 600 MHz) δ 8.88 (s, 1H), 8.32 (s, 1H), 7.56–7.48 (m, 3H), 7.45–7.39 (m, 2H), 7.36 (s, 1H), 7.33 (d, J = 7.8 Hz, 2H), 7.01 (dd, J = 9.0, 1.2 Hz, 1H), 6.76 (br s, 1H), 6.43 (d, J = 16.2 Hz, 1H), 4.32 (d, J = 4.2 Hz, 2H), 3.87 (s, 3H). HRMS calcd for $C_{21}H_{21}N_4O_5$ 409.1506 $(M+H)^+$, found 409.1500.

4.2.20. Hydroxamic acid 16b

Following procedures similar to those described for hydroxamic acid **16a**, protected hydroxamate **28b** (56 mg, 0.086 mmol) was converted into hydroxamic acid **16b** as a pale solid (34 mg, 97%) ^{1}H NMR (DMSO-d_6, 600 MHz) δ 8.86 (s, 1H), 8.32 (s, 1H), 7.54 (d, J = 8.4 Hz, 1H), 7.48 (s, 1H), 7.46–7.40 (m, 3H), 7.38 (d, J = 7.8 Hz, 1H), 7.36 (s, 1H), 7.31 (d, J = 7.8 Hz, 1H), 7.02 (d, J = 8.4 Hz, 1H), 6.77 (br s, 1H), 6.45 (d, J = 15.6 Hz, 1H), 4.32 (d, J = 4.2 Hz, 2H), 3.87 (s, 3H). HRMS calcd for $C_{21}H_{21}N_4O_5$ 409.1506 $(M+H)^+$, found 409.1506.

4.2.21. Hydroxamic acid 16c

Following procedures similar to those described for hydroxamic acid **16a**, protected hydroxamate **28c** (300 mg, 0.49 mmol) was converted into hydroxamic acid **16c** as a pale solid (150 mg, 83%). ^{1}H NMR (DMSO-d_6, 600 MHz) δ 9.22 (s, 1H), 7.55–7.48 (m, 3H), 7.46 (s, 1H), 7.42 (d, J = 15.6 Hz, 1H), 7.32 (d, J = 7.2 Hz, 2H), 6.98 (d, J = 8.4 Hz, 1H), 6.93 (s, 1H), 6.42 (d, J = 15.6 Hz, 1H), 4.31 (d, J = 4.2 Hz, 2H), 3.83 (s, 3H). HRMS calcd for $C_{19}H_{19}N_4O_4$ 367.1406 $(M+H)^+$, found 367.1387.

4.2.22. Hydroxamic acid 16d

Following procedures similar to those described for hydroxamic acid **16a**, protected hydroxamate **28d** (300 mg, 0.49 mmol) was converted into hydroxamic acid **16d** as a pale solid (103 mg, 57%). ^{1}H NMR (DMSO-d_6, 600 MHz) δ 9.21 (s, 1H), 7.51 (d, J = 9.0 Hz, 1H), 7.48–7.40 (m, 4H), 7.37 (t, J = 7.5 Hz, 1H), 7.30 (d, J = 7.2 Hz, 1H), 6.99 (d, J = 8.4 Hz, 1H), 6.94 (t, J = 6.0 Hz, 1H), 6.44 (d, J = 15.6 Hz, 1H), 4.32 (d, J = 5.4 Hz, 2H), 3.83 (s, 3H). HRMS calcd for $C_{19}H_{19}N_4O_4$ 367.1406 $(M+H)^+$, found 367.1380.

4.2.23. *tert*-Butyl ester 30a

A solution of (*E*)-*tert*-butyl 3-(4-(aminomethyl)phenyl)acrylate hydrochloride (405 mg, 1.50 mmol), 2-(3-methoxy-4-(oxazol-5-yl)phenylamino)-2-oxoacetic acid[21] (472 mg, 1.80 mmol), PyBOP (1.17 g, 2.25 mmol) and NMM (0.66 mL, 6.00 mmol) in anhydrous DMF (15 mL) was stirred at rt for 48 h. The reaction mixture was slowly added to ice/water (150 mL plus 20 mL of 1 N HCl). The solid precipitate was washed with water, collected and purified by silica gel column chromatography (30–50% EtOAc/hexanes) to give

tert-butyl ester **30a** as a yellow solid (298 mg, 42%). ^{1}H NMR ($CDCl_3$, 600 MHz) δ 9.38 (s, 1H), 7.92 (t, J = 5.7 Hz, 1H), 7.90 (s, 1H), 7.75 (d, J = 7.8 Hz, 1H), 7.60–7.54 (m, 2H), 7.53 (s, 1H), 7.50 (d, J = 8.4 Hz, 2H), 7.32 (d, J = 8.4 Hz, 2H), 7.17 (dd, J = 8.4, 1.8 Hz, 1H), 6.36 (d, J = 15.6 Hz, 1H), 4.58 (d, J = 6.0 Hz, 2H), 3.98 (s, 3H), 1.54 (s, 9H). HRMS calcd for $C_{26}H_{27}N_3O_6Na$ 500.1792 $(M+Na)^+$, found 500.1793.

4.2.24. *tert*-Butyl ester 30b

Following procedures similar to those described for *tert*-butyl ester **30a**, (*E*)-*tert*-butyl 3-(3-(aminomethyl)phenyl)acrylate hydrochloride (405 mg, 1.50 mmol) was converted into *tert*-butyl ester **30b** as a yellow solid (305 mg, 42%). ^{1}H NMR ($CDCl_3$, 600 MHz) δ 9.38 (s, 1H), 7.92 (t, J = 5.7 Hz, 1H), 7.90 (s, 1H), 7.76 (d, J = 8.4 Hz, 1H), 7.60–7.52 (m, 3H), 7.48–7.42 (m, 2H), 7.37 (t, J = 7.5 Hz, 1H), 7.31 (d, J = 7.8 Hz, 2H), 7.18 (dd, J = 8.4, 1.8 Hz, 1H), 6.38 (d, J = 16.2 Hz, 1H), 4.58 (d, J = 6.0 Hz, 2H), 3.98 (s, 3H), 1.53 (s, 9H). HRMS calcd for $C_{26}H_{27}N_3O_6Na$ 500.1792 $(M+Na)^+$, found 500.1797.

4.2.25. Carboxylic acid 31a

A solution of *tert*-butyl ester **30a** in dry CH_2Cl_2 (6 mL) and TFA (6 mL) was allowed to stir at rt overnight and then concentrated. After co-evaporation with toluene, carboxylic acid **31a** was obtained as a yellow solid (240 mg, 100%). ^{1}H NMR (DMSO-d_6, 600 MHz) δ 10.79 (s, 1H), 9.59 (t, J = 6.6 Hz, 1H), 8.38 (s, 1H), 7.75 (s, 1H), 7.68–7.61 (m, 4H), 7.56 (d, J = 15.6 Hz, 1H), 7.47 (s, 1H), 7.34 (d, J = 8.4 Hz, 2H), 6.49 (d, J = 16.2 Hz, 1H), 4.42 (d, J = 6.0 Hz, 2H), 3.90 (s, 3H). HRMS calcd for $C_{22}H_{20}N_3O_6$ 422.1346 $(M+H)^+$, found 422.1350.

4.2.26. Carboxylic acid 31b

Following procedures similar to those described for carboxylic acid **31a**, *tert*-butyl ester **30b** (280 mg, 0.59 mmol) was converted into carboxylic acid **31b** as a yellow solid (240 mg, 97%). ^{1}H NMR (DMSO-d_6, 600 MHz) δ 10.79 (s, 1H), 9.56 (t, J = 6.3 Hz, 1H), 8.38 (s, 1H), 7.76 (s, 1H), 7.69–7.60 (m, 3H), 7.60–7.53 (m, 2H), 7.47 (s, 1H), 7.40–7.32 (m 2H), 6.50 (d, J = 16.2 Hz, 1H), 4.43 (d, J = 6.0 Hz, 2H), 3.90 (s, 3H). HRMS calcd for $C_{22}H_{20}N_3O_6$ 422.1346 $(M+H)^+$, found 422.1346.

4.2.27. Protected hydroxamate 32a

A solution of carboxylic acid **31a** (215 mg, 0.51 mmol), EDC (310 mg, 1.57 mmol), HOBt (139 mg, 1.03 mmol) and *O*-tritylhydroxylamine (281 mg, 1.02 mmol) in anhydrous DMF (15 mL) was stirred at rt for 4 d. After concentration, the residue was dissolved in MeOH (15 mL) and slowly added to ice/water (150 mL). The solid precipitate was washed with water, collected and purified by silica gel column chromatography (0–4% MeOH/CH_2Cl_2) to give protected hydroxamate **32a** as a light-yellow solid (281 mg, 81%). ^{1}H NMR ($CDCl_3$, 600 MHz) δ 9.38 (s, 1H), 7.94–7.86 (m, 2H), 7.75 (d, J = 7.8 Hz, 1H), 7.57 (d, J = 1.2 Hz, 1H), 7.53 (s, 1H), 7.43 (br s, 5H), 7.36–7.31 (m, 7H), 7.31–7.26 (m, 4H), 7.24 (d, J = 7.8 Hz, 2H), 7.18 (dd, J = 8.7, 1.5 Hz, 1H), 6.09 (d, J = 16.2 Hz, 1H), 4.54 (d, J = 6.6 Hz, 2H), 3.98 (s, 3H). HRMS calcd for $C_{41}H_{34}N_4O_6Na$ 701.2370 $(M+Na)^+$, found 701.2366.

4.2.28. Protected hydroxamate 32b

Following procedures similar to those described for protected hydroxamate **32a**, carboxylic acid **31b** (215 mg, 0.51 mmol) was converted into protected hydroxamate **32b** as a light-yellow solid (200 mg, 58%). ^{1}H NMR ($CDCl_3$, 600 MHz) δ 9.35 (s, 1H), 7.93–7.84 (m, 2H), 7.76 (d, J = 8.4 Hz, 1H), 7.56 (d, J = 1.8 Hz, 1H), 7.53 (s, 1H), 7.43 (br s, 5H), 7.36–7.31 (m, 7H), 7.30–7.23 (m, 6H), 7.16 (dd, J = 8.1, 1.5 Hz, 1H), 6.10 (d, J = 15.6 Hz, 1H), 4.53 (d, J = 6.0 Hz, 2H), 3.97 (s, 3H). HRMS calcd for $C_{41}H_{34}N_4O_6Na$ 701.2370 $(M+Na)^+$, found 701.2369.

4.2.29. Hydroxamic acid 17a

To a solution of protected hydroxamate **32a** (250 mg, 0.37 mmol) in anhydrous CH_2Cl_2 (10 mL) was added TFA (0.50 mL). The resulting yellow solution was treated with Et_3SiH till there was no change of color. After stirring for additional 30 min, the solid precipitate was filtered, washed with CH_2Cl_2 and collected to give hydroxamic acid **17a** as a yellowish solid (151 mg, 94%). ^{1}H NMR (DMSO-d_6, 600 MHz) δ 10.79 (s, 1H), 9.58 (t, J = 6.3 Hz, 1H), 8.39 (s, 1H), 7.75 (s, 1H), 7.68–7.61 (m, 2H), 7.52 (d, J = 7.8 Hz, 2H), 7.48 (s, 1H), 7.42 (d, J = 16.2 Hz, 1H), 7.33 (d, J = 7.8 Hz, 2H), 6.43 (d, J = 15.6 Hz, 1H), 4.41 (d, J = 6.6 Hz, 2H), 3.90 (s, 3H). HRMS calcd for $C_{22}H_{21}N_4O_6$ 437.1455 $(M+H)^+$, found 437.1451.

4.2.30. Hydroxamic acid 17b

Following procedures similar to those described for hydroxamic acid **17a**, protected hydroxamate **32b** (175 mg, 0.26 mmol) was converted into hydroxamic acid **17b** as a pale solid (105 mg, 93%). ^{1}H NMR (DMSO-d_6, 600 MHz) δ 10.79 (s, 1H), 9.58 (t, J = 6.0 Hz, 1H), 8.38 (s, 1H), 7.76 (s, 1H), 7.69–7.61 (m, 2H), 7.50 (s, 1H), 7.48 (s, 1H), 7.46–7.40 (m, 2H), 7.37 (t, J = 7.5 Hz, 1H), 7.31 (d, J = 7.2 Hz, 1H), 6.45 (d, J = 15.6 Hz, 1H), 4.42 (d, J = 6.6 Hz, 2H), 3.91 (s, 3H). HRMS calcd for $C_{22}H_{21}N_4O_6$ 437.1455 $(M+H)^+$, found 437.1450.

4.2.31. Ethyl ester 34a

To a solution of 3-methoxy-4-(oxazol-5-yl) aniline (570 mg, 3.0 mmol) and triphosgene (296 mg, 1.0 mmol) in CH_2Cl_2 (10 mL) was added Et_3N (0.50 mL, 5.0 mmol) at 5 °C and the mixture was refluxed for 2.5 h. The mixture was cooled to room temperature and a solution of ethyl 4-aminocinnamate hydrochloride (**33a**, 555 mg, 2.0 mmol) in CH_2Cl_2 was added. Additional Et_3N (0.25 mL) was added and the mixture was stirred at rt for 2.5 h and then poured into water. The product was extracted with EtOAc and purified on silica gel column (Hexanes/EtOAc/MeOH = 6:3:1) to obtain ethyl ester **34a** (410 mg, 50%). ^{1}H NMR (DMSO-d_6, 600 MHz): δ 9.91 (s, 1H), 8.99 (s, 1H), 8.36 (s, 1H), 7.65 (d, J = 8.4 Hz, 2H), 7.61 (d, J = 8.4 Hz, 1H), 7.58 (d, J = 16.2 Hz, 1H), 7.52 (d, J = 8.4 Hz, 2H), 7.46 (s, 1H), 7.42 (s, 1H), 7.08 (dd, J = 8.4, 1.2 Hz, 1H), 6.48 (d, J = 16.2 Hz, 1H), 4.18 (q, J = 7.2 Hz, 2H), 3.93 (s, 3H), 1.25 (t, J = 7.2 Hz, 1H). ^{13}C NMR (DMSO-d_6): δ 167.1, 156.5, 152.8, 150.9, 147.9, 144.8, 142.4, 141.7, 130.0, 128.4, 126.6, 124.1, 118.8, 116.3, 111.1, 110.8, 101.8, 102.1, 60.5, 56.1, 14.9. HRMS calcd for $C_{22}H_{21}N_3O_5Na$ 430.1373 $(M+Na)^+$, found 430.1385.

4.2.32. Ethyl ester 34b

Following procedures similar to those described for ethyl ester **34a**, 3-methoxy-4-(oxazol-5-yl) aniline (**24**, 570 mg, 3.0 mmol) and ethyl 3-aminocinnamate (**33b**, 382 mg, 2.0 mmol) were combined to give ethyl ester **34b** (220 mg, 27%). ^{1}H NMR (DMSO-d_6, 600 MHz): δ 8.13 (s, 1H), 7.71 (s, 1H), 7.57 (d, J = 8.4 Hz, 2H), 7.56 (d, J = 15.6 Hz, 1H), 7.44 (s, 1H), 7.40 (d, J = 7.2 Hz, 1H), 7.34 (d, J = 1.2 Hz, 1H), 7.28 (t, J = 7.8 Hz, 1H), 7.21 (d, J = 7.8 Hz, 1H), 6.97 (d, J = 8.4 Hz, 1H), 6.43 (d, J = 15.6 Hz, 1H), 4.14 (q, J = 7.2 Hz, 2H), 3.89 (s, 3H), 1.22 (t, J = 7.2 Hz, 3H). ^{13}C NMR (DMSO-d_6): δ 166.8, 156.6, 153.1, 150.3, 148.2, 144.7, 141.5, 140.3, 135.3, 129.7, 126.3, 123.5, 122.5, 120.9, 118.6, 118.1, 110.9, 110.8, 101.8, 60.5, 55.3, 13.9. HRMS calcd for $C_{22}H_{22}N_3O_5$ 408.1553 $(M+H)^+$, found 408.1561.

4.2.33. Ethyl ester 34c

Following procedures similar to those described for ethyl ester **34a**, 4-cyano-3-methoxy aniline hydrochloride (**25**, 554 mg, 3.0 mmol) and ethyl 4-aminocinnamate hydrochloride (**33a**, 555 mg, 2.0 mmol) were combined to give ethyl ester **34c**

(710 mg, 97%). ^{1}H NMR (DMSO-d_6, 600 MHz): δ 9.29 (s, 1H), 9.11 (s, 1H), 7.66 (d, J = 8.4 Hz, 2H), 7.59 (d, J = 15.6 Hz, 1H), 7.58 (d, J = 7.2 Hz, 1H), 7.52 (d, J = 9.0 Hz, 2H), 7.49 (s, 1H), 7.04 (d, J = 8.4 Hz, 1H), 6.50 (d, J = 15.6 Hz, 1H), 4.17 (q, J = 7.2 Hz, 2H), 3.88 (s, 3H), 1.25 (t, J = 7.2 Hz, 1H). ^{13}C NMR (DMSO-d_6): δ 167.1, 162.4, 152.5, 146.4, 144.8, 141.9, 134.8, 130.0, 128.7, 119.0, 117.6, 116.6, 111.1, 101.5, 93.5, 60.5, 56.6, 14.9. HRMS calcd for $C_{20}H_{19}N_3O_4Na$ 388.1267 $(M+Na)^+$, found 388.1281.

4.2.34. Ethyl ester 34d

Following procedures similar to those described for ethyl ester **34a**, 4-cyano-3-methoxy aniline hydrochloride (**25**, 369 mg, 2.0 mmol) and ethyl 3-aminocinnamate (**33b**, 573 mg, 3.0 mmol) were combined to give ethyl ester **34d** (485 mg, 66%). ^{1}H NMR (DMSO-d_6, 600 MHz): δ 9.29 (s, 1H), 8.90 (s, 1H), 7.74 (s, 1H), 7.60 (d, J = 15.6 Hz, 1H), 7.57 (d, J = 9.0 Hz, 1H), 7.50 (s, 1H), 7.48 (d, J = 6.6 Hz, 1H), 7.38 (d, J = 7.2 Hz, 1H), 7.35 (t, J = 6.8 Hz, 1H), 7.01 (dd, J = 7.8, 1.2 Hz, 1H), 6.52 (d, J = 16.2 Hz, 1H), 4.16 (q, J = 7.2 Hz, 2H), 3.87 (s, 3H), 1.25 (t, J = 7.2 Hz, 1H). ^{13}C NMR (DMSO-d_6): δ 166.0, 161.7, 152.1, 145.9, 144.3, 139.6, 134.6, 134.1, 129.4, 122.2, 120.7, 118.4, 118.3, 116.9, 110.3, 100.7, 92.7, 60.1, 55.9, 14.1. HRMS calcd for $C_{20}H_{19}N_3O_4Na$ 388.1267 $(M+Na)^+$, found 388.1284.

4.2.35. Carboxylic acid 35a

To a suspension of ethyl ester **34a** (300 mg, 0.74 mmol) in THF (5 mL) were added methanol (2.5 mL) and NaOH (590 mg, 15 mmol in 5 mL of water). The mixture was stirred at room temperature overnight. After solvents were removed, the residue was diluted with water and pH was adjusted with aqueous HCl to 1–2. The precipitate of the product was filtered, collected and dried to give carboxylic acid **35a** (245 mg, 87%). ^{1}H NMR (DMSO-d_6, 600 MHz): δ 9.01 (br s, 2H), 8.34 (s, 1H), 7.53–7.61 (m, 5H), 7.45 (d, J = 16.2 Hz, 1H), 7.48–7.56 (m, 2H), 7.08 (d, J = 6.6 Hz, 1H), 6.40 (d, J = 16.2 Hz, 1H), 3.92 (s, 3H). ^{13}C NMR (DMSO-d_6): δ 168.5, 156.5, 152.9, 150.9, 147.9, 146.7, 144.5, 142.2, 141.8, 129.9, 128.6, 126.6, 124.1, 118.8, 117.4, 113.4, 111.1, 110.9, 102.1, 56.2. HRMS calcd for $C_{20}H_{18}N_3O_5$ 380.1240 $(M+H)^+$, found 380.1233.

4.2.36. Carboxylic acid 35b

Following procedures similar to those described for carboxylic acid **35a**, ethyl ester **34b** (580 mg, 1.43 mmol) underwent hydrolysis to give carboxylic acid **35b** (360 mg, 66%). ^{1}H NMR (DMSO-d_6, 600 MHz): δ 9.91 (s, 1H), 9.80 (s, 1H), 8.34 (s, 1H), 7.76 (s, 1H), 7.58 (d, J = 7.2 Hz, 1H), 7.56 (d, J = 14.4 Hz, 1H), 7.48–7.56 (m, 2H), 7.40 (s,1H), 7.29–7.31 (m, 2H), 7.05 (d, J = 6.8 Hz, 1H), 6.43 (d, J = 15.6 Hz, 1H), 3.91 (s, 3H). ^{13}C NMR (DMSO-d_6): δ 166.9, 155.3, 152.2, 149.7, 146.8, 143.5, 141.0, 139.8, 134.2, 128.9, 125.4, 122.7, 121.3, 119.4, 118.7, 116.6, 109.6, 109.3, 100.4, 54.9. HRMS calcd for $C_{20}H_{18}N_3O_5$ 380.1240 $(M+H)^+$, found 380.1233.

4.2.37. Carboxylic acid 35c

Following procedures similar to those described for carboxylic acid **35a**, ethyl ester **34c** (365 mg, 1.0 mmol) underwent hydrolysis to give carboxylic acid **35c** as a yellow solid (330 mg, 98%). ^{1}H NMR (DMSO-d_6, 600 MHz): δ 12.2 (br s, 1H), 10.1 (br s, 1H), 9.91 (br s, 1H), 7.62 (d, J = 8.4 Hz, 2H), 7.58 (d, J = 8.4 Hz, 1H), 7.49–7.53 (m, 4H), 7.02 (dd, J = 8.4, 1.2 Hz, 1H), 6.40 (d, J = 16.2 Hz, 1H), 3.88 (s, 3H). ^{13}C NMR (DMSO-d_6): δ 168.5, 162.4, 152.8, 146.6, 144.4, 141.9, 134.8, 129.9, 118.7, 117.7, 117.5, 113.4, 110.8, 101.1, 93.3, 56.6. HRMS calcd for $C_{18}H_{15}N_3O_4Na$ 360.0954 $(M+Na)^+$, found 360.0965.

4.2.38. Carboxylic acid 35d

Following procedures similar to those described for carboxylic acid **35a**, ethyl ester **34d** (365 mg, 1.0 mmol) underwent hydrolysis to give carboxylic acid **35d** (250 mg, 74%). ^{1}H NMR (DMSO-d_6, 600 MHz): δ 6.99 (s, 1H), 6.83 (d, J = 15.6 Hz, 1H), 6.79 (s, 1H), 6.72 (t, J = 10.2, 8.4 Hz, 2H), 6.58 (t, J = 7.8 Hz, 1H), 6.51 (d, J = 7.2 Hz, 1H), 6.23 (d, J = 10.2 Hz, 1H), 5.70 (d, J = 15.6 Hz, 1H), 4.16 (q, J = 7.2 Hz, 2H), 3.78 (s, 3H). ^{13}C NMR (DMSO-d_6): δ 168.8, 162.7, 153.1, 146.4, 144.8, 140.1, 135.7, 134.4, 129.8, 123.0, 121.2, 119.5, 118.5, 117.2, 110.9, 101.4, 94.1, 55.9. HRMS calcd for $C_{18}H_{15}N_3O_4Na$ 360.0954 $(M+Na)^+$, found 360.0963.

4.2.39. Hydroxamic acid 18a

To a solution of carboxylic acid **35a** (100 mg, 0.26 mmol) in dried DMF (5 mL) were added *O*-tritylhydroxylamine (109 mg, 1.5 mmol), EDC (101 mg, 0.52 mmol) and 1-hydroxybenzotriazole (53 mg, 0.40 mmol). The mixture was stirred at room temperature overnight. Solvent was removed and the residue was purified on silica gel column ($CHCl_3$: MeOH = 9: 1) to give protected hydroxamate **36a** (70 mg, 42%). To a portion of **36a** (64 mg, 0.10 mmol) in CH_2Cl_2 (5 mL) was added TFA (0.25 mL) and triethylsilane (0.25 mL). The mixture was allowed to stir overnight. The precipitate was filtered, collected and dried to give hydroxamic acid **18a** (38 mg, 96%). ^{1}H NMR (DMSO-d_6, 600 MHz): δ 9.05 (s, 1H), 9.00 (s, 1H), 8.36 (s, 1H), 7.60 (d, J = 8.4 Hz, 1H), 7.48–7.53 (m, 5H), 7.42 (d, J = 12.0 Hz, 1H), 7.39 (d, J = 10.2 Hz, 1H), 7.07 (d, J = 8.4 Hz, 1H), 6.35 (d, J = 15.6 Hz, 1H), 3.92 (s, 3H). ^{13}C NMR (DMSO-d_6): δ 213.6, 180.2, 156.4, 152.8, 146.7, 141.8, 129.0, 126.6, 118.9, 113.3, 111.0, 110.8, 102.2, 56.1. HRMS calcd for $C_{20}H_{19}N_4O_5$ 395.1349 $(M+H)^+$, found 395.1331.

4.2.40. Hydroxamic acid 18b

Following procedures similar to those described for hydroxamic acid **18a**, carboxylic acid **35b** (100 mg, 0.26 mmol) was converted into protected hydroxamate **36b** (90 mg, 54%). A portion of **36b** (64 mg, 0.10 mmol) was deprotected to give hydroxamic acid **18b** (37 mg, 93%). ^{1}H NMR (DMSO-d_6, 600 MHz): δ 9.02 (s, 1H), 8.87 (s, 1H), 8.35 (s, 1H), 7.78 (s, 1H), 7.61 (d, J = 9.0 Hz, 1H), 7.38–7.45 (m, 4H), 7.32 (t, J = 7.8 Hz, 2H), 7.17 (d, J = 7.8 Hz, 1H), 7.08 (d, J = 7.8 Hz, 1H), 6.43 (d, J = 16.2 Hz, 1H), 3.92 (s, 3H). ^{13}C NMR (DMSO-d_6): δ 162.6, 158.5, 152.4, 150.2, 147.2, 141.2, 140.0, 138.4, 135.4, 129.4, 125.9, 123.3, 121.8, 119.6, 116.5, 110.3, 110.0, 101.3, 55.4. HRMS calcd for $C_{20}H_{19}N_4O_5$ 395.1349 $(M+H)^+$, found 395.1339.

4.2.41. Hydroxamic acid 18c

Following procedures similar to those described for hydroxamic acid **18a**, carboxylic acid **35c** (100 mg, 0.30 mmol) was converted into protected hydroxamate **36c** (85 mg, 48%). A portion of **36c** (60 mg, 0.10 mmol) was deprotected to give hydroxamic acid **18c** (25 mg, 71%). ^{1}H NMR (DMSO-d_6, 600 MHz): δ 10.7 (s, 1H), 9.31 (s, 1H), 9.10 (s, 1H), 8.98 (s, 1H), 7.59 (d, J = 9.0 Hz, 1H), 7.50 (br s, 5H), 7.40 (d, J = 15.6 Hz, 1H), 7.03 (d, J = 8.4 Hz, 1H), 6.35 (d, J = 16.2 Hz, 1H), 3.88 (s, 3H). ^{13}C NMR (DMSO-d_6): δ 162.4, 152.6, 146.7, 146.5, 141.0, 138.7, 134.8, 129.6, 129.0, 119.2, 117.6, 113.3, 111.0, 101.4, 93.4, 56.6. HRMS calcd for $C_{18}H_{16}N_4O_4Na$ 375.1063 $(M+Na)^+$, found 375.1065.

4.2.42. Hydroxamic acid 18d

Following procedures similar to those described for hydroxamic acid **18a**, carboxylic acid **35d** (100 mg, 0.30 mmol) was converted into protected hydroxamate **36d**. A portion of **36d** (60 mg, 0.10 mmol) was deprotected to give hydroxamic acid **18d** (32 mg, 90%). ^{1}H NMR (DMSO-d_6, 600 MHz): δ 9.30 (s, 1H), 8.99 (s, 1H), 7.76 (s, 1H), 7.58 (d, J = 8.4 Hz, 1H), 7.48 (s, 1H), 7.41 (d, J = 15.6 Hz, 1H), 7.39 (d, J = 11.4 Hz, 1H), 7.33 (t, J = 7.8, 7.2 Hz, 1H), 7.19 (d, J = 7.8 Hz, 1H), 7.04 (d, J = 8.4 Hz, 1H), 6.43 (d, J = 15.6 Hz, 1H), 3.88 (s, 3H). ^{13}C NMR (DMSO-d_6): δ 161.7, 152.1, 145.9, 139.6, 138.3, 135.4, 134.1, 129.4, 122.1, 119.8, 119.2,

116.9, 116.8, 110.3, 100.7, 92.7, 55.9. HRMS calcd for $C_{18}H_{16}N_4O_4$-Na 375.1063 $(M+Na)^+$, found 375.1055.

4.2.43. Ethyl ester 37a

To a solution of 2-(3-methoxy-4-(oxazol-5-yl)phenylamino)-2-oxoacetic acid (**29**, 600 mg, 2.29 mmol) in anhydrous DMF (15 mL) were added benzotriazol-1-yloxy-tripyrrolidinophosphonium hexafluorophosphate (PyBOP) (2.38 g, 4.56 mmol), 4-methylmorpholine (NMM) (1.10 mL, 9.16 mmol) and (*E*)-ethyl 3-(4-aminophenyl)acrylate (**33a**, 525 mg, 2.75 mmol). The mixture was stirred at rt for 48 h. After concentration, the resulting residue was diluted with EtOAC (50 mL) and subsequently washed with H_2O (2 × 10 mL) and brine (2 × 10 mL). The organic layer was dried over Na_2SO_4 and filtered. The filtrate was concentrated and the residue was purified by flash chromatography column (0–3% MeOH/CH_2Cl_2) to give ethyl ester **37a** as a light-yellow solid (500 mg, 50%). Mp = 187.6–188.1 °C. ^{1}H NMR (DMSO-d_6, 600 MHz): δ 11.04 (s, 1H), 11.01 (s, 1H), 8.38 (s, 1H), 7.91 (d, J = 8.51 Hz, 1H), 7.82 (s, 1H), 7.72 (d, J = 8.2 Hz, 1H), 7.67 (d, J = 8.5 Hz, 2H), 7.63 (d, J = 8.2 Hz, 2H), 7.61 (d, J = 16.1 Hz, 1H), 7.48 (s, 1H), 6.58 (d, J = 15.8 Hz, 1H), 4.17 (q, J = 6.7 Hz, 2H), 3.91 (s, 3H), 1.23 (t, J = 6.3 Hz, 3H). HRMS calcd for $C_{23}H_{22}N_3O_6$ 436.2054 $(M+H)^+$, found 436.2058.

4.2.44. Ethyl ester 37b

Following procedures similar to those described for ethyl ester **37a**, oxoacetic acid **29** (200 mg, 0.763 mmol) in anhydrous DMF (4 mL) was treated with PyBOP (790 mg, 1.52 mmol), NMM (0.33 mL, 3.05 mmol) and (*E*)-ethyl 3-(3-aminophenyl)acrylate (**33b**, 175 mg, 0.92 mmol) to give ethyl ester **37b** as a pale solid (210 mg, 65%). Mp = 185.7–187.1 °C. ^{1}H NMR (DMSO-d_6, 600 MHz): δ 10.98 (s, 1H), 10.91 (s, 1H), 8.38 (s, 1H), 8.10 (s, 1H), 7.92 (d, J = 6.7 Hz, 1H), 7.81 (s, 1H), 7.68 (d, J = 7.9 Hz, 1H), 7.66 (d, J = 7.6 Hz, 1H), 7.59 (d, J = 16.1 Hz, 1H), 7.51 (d, J = 7.1 Hz, 1H), 7.47 (s, 1H), 6.53 (d, J = 15.8 Hz, 1H), 4.17 (q, J = 6.7 Hz, 2H), 3.91 (s, 3H), 1.24 (t, J = 6.3 Hz, 3H). ^{13}C NMR (DMSO-d_6, 150 MHz): δ 166.8, 165.3, 156.6, 153.1, 150.3, 148.2, 144.7, 141.5, 140.3, 135.3, 129.7, 126.3, 123.5, 122.5, 120.9, 118.6, 118.1, 110.9, 110.8, 101.8, 60.5, 55.3, 13.9. HRMS calcd for $C_{23}H_{22}N_3O_6$ 436.1433 $(M+H)^+$, found 436.1439.

4.2.45. Carboxylic acid 38a

To a suspension of ethyl ester **37a** (450 mg, 1.03 mmol) in THF (18 mL) were added methanol (6 mL) and NaOH (910 mg in 18 mL water). The mixture was stirred at room temperature overnight. Solvents were removed and the residue was diluted with water and 1 N HCl was added until pH ≈ 1–2. The solid that formed was collected by filtration and dried to carboxylic acid **38a** as a white solid (260 mg, 62%). Mp = 184.2–185.7 °C. ^{1}H NMR (DMSO-d_6, 600 MHz): δ 12.07 (br s, 1H), 10.85 (s, 1H), 10.82 (s, 1H), 8.37 (s, 1H), 7.81 (d, J = 8.2 Hz, 1H), 7.66 (d, J = 4.4 Hz, 2H), 7.64 (s, 1H), 7.62 (d, J = 8.4 Hz, 2H), 7.54 (d, J = 8.5 Hz, 1H), 7.51 (d, J = 15.8 Hz, 1H), 7.45 (s, 1H), 6.44 (d, J = 16.1 Hz, 1H), 3.91 (s, 3H). HRMS calcd for $C_{21}H_{18}N_3O_6$ 408.1233 $(M+H)^+$, found 408.1236.

4.2.46. Carboxylic acid 38b

Following procedures similar to those described for carboxylic acid **38a**, ethyl ester **37b** (210 mg, 0.48 mmol) in THF (6 mL) was treated with methanol (3 mL) and NaOH (0.29 g in 6 mL water) to give carboxylic acid **38b** as a light-yellow solid (150 mg, 77%). Mp = 188.5–189.3 °C. ^{1}H NMR (DMSO-d_6, 600 MHz): δ 12.44 (br s, 1H), 10.99 (s, 1H), 10.91 (s, 1H), 8.37 (s, 1H), 8.09 (s, 1H), 7.89 (d, J = 7.9 Hz, 1H), 7.81 (s, 1H), 7.67 (d, J = 7.9 Hz, 2H), 7.65 (d, J = 7.6 Hz, 1H), 7.53 (d, J = 16.4 Hz, 1H), 7.47 (s, 1H), 7.42 (d, J = 7.3 Hz, 1H), 6.43 (d, J = 15.8 Hz, 1H), 3.95 (s, 3H). ^{13}C NMR (DMSO-d_6, 150 MHz): δ 166.9, 165.2, 155.3, 152.2, 149.7, 146.8, 143.5, 141.0, 139.8, 134.2, 128.9, 125.4, 122.7, 121.3, 119.4, 118.7, 116.6, 109.6, 109.3, 100.4, 54.9. HRMS calcd for $C_{21}H_{18}N_3O_6$ 408.1051 $(M+H)^+$, found 408.1053.

4.2.47. Protected hydroxamate 39a

A solution of carboxylic acid **38a** (250 mg, 0.61 mmol), *O*-tritylhydroxylamine (277 mg, 1.22 mmol), EDC (295 mg, 1.53 mmol), and HOBt (166 mg, 1.22 mmol) in anhydrous DMF (20 mL) was stirred at rt for 24 h. After concentration, the residue was diluted with EtOAc (25 mL) and washed with water (2 × 15 mL) and brine (2 × 20 mL). The organic layer was dried over Na_2SO_4 and filtered. The filtrate was concentrated and the residue was purified by flash column chromatography (0–5% MeOH/CH_2Cl_2) to give protected hydroxamate **39a** as a white solid (210 mg, 52%). Mp = 209.5–211.1 °C. ^{1}H NMR (DMSO-d_6, 600 MHz): δ 11.09 (s, 1H), 11.05 (s, 1H), 10.61 (s, 1H), 8.38 (s, 1H), 7.82 (s, 1H), 7.67 (s, 1H), 7.66 (d, J = 8.4 Hz, 2H), 7.64 (s, 1H), 7.61 (d, J = 7.1 Hz, 2H), 7.48 (s, 1H), 7.43 (d, J = 15.7 Hz, 1H), 7.38–7.23 (m, 15H), 6.44 (d, J = 15.5 Hz, 1H), 3.95 (s, 3H). HRMS calcd for $C_{40}H_{33}N_4O_6$ 665.2642 $(M+H)^+$, found 665.2649.

4.2.48. Protected hydroxamate 39b

Following procedures similar to those described for protected hydroxamate **39a**, carboxylic acid **38b** (120 mg, 0.29 mmol) in anhydrous DMF (10 mL) was treated with H_2N-OTr (135 mg, 0.59 mmol), EDC (142 mg, 0.73 mmol), and HOBt (80 mg, 0.59 mmol) to give protected hydroxamate **39b** as a white solid (70 mg, 55%). Mp = 218.5–219.2 °C. ^{1}H NMR (DMSO-d_6, 600 MHz): δ 10.94 (s, 1H), 10.89 (s, 1H), 10.46 (s, 1H), 8.36 (s, 1H), 7.98 (s, 1H), 7.92 (s, 1H), 7.79–7.77 (m, 2H), 7.67 (d, J = 8.5 Hz, 1H), 7.62 (d, J = 8.8 Hz, 1H), 7.48 (s, 1H), 7.41 (d, J = 16.4 Hz, 1H), 7.39–7.18 (m, 15H), 6.44 (d, J = 15.5 Hz, 1H), 3.91 (s, 3H). HRMS calcd for $C_{40}H_{33}N_4O_6$ 665.2332 $(M+H)^+$, found 665.2337.

4.2.49. Hydroxamic acid 19a

To a solution of protected hydroxamate **39a** (70 mg, 0.10 mmol) in anhydrous CH_2Cl_2 (6 mL) was added TFA (0.15 mL). The resulting yellow solution was treated with Et_3SiH till it was colorless. After being stirring for an additional 30 min, the solid formed was filtered, washed with anhydrous CH_2Cl_2 and dried under high vacuum to give hydroxamic acid **19a** as a light-yellow solid (9.3 mg, 22%). Mp = 174.3–175.9 °C. ^{1}H NMR (DMSO-d_6, 600 MHz): δ 11.01 (s, 1H), 10.96 (s, 1H), 10.83 (s, 1H), 8.39 (s, 1H), 8.05 (s, 1H), 7.87 (d, J = 7.9 Hz, 1H), 7.83 (s, 1H), 7.65 (d, J = 8.5 Hz, 2H), 7.62 (d, J = 8.2 Hz, 2H), 7.49 (s,1H), 7.43 (d, J = 15.7 Hz, 1H), 7.37 (d, J = 7.7 Hz, 1H), 6.39 (d, J = 15.9 Hz, 1H), 3.92 (s, 3H). HRMS calcd for $C_{21}H_{19}N_4O_6$ 423.1292 $(M+H)^+$, found 423.1310.

4.2.50. Hydroxamic acid 19b

Following procedures similar to those described for hydroxamic acid **19a**, protected hydroxamate **39b** (50 mg, 0.075 mmol) in anhydrous CH_2Cl_2 (6 mL) was treated with TFA (0.1 mL) to give hydroxamic acid **19b** as a white solid (7.5 mg, 25%). Mp = 173.5–174.8 °C. ^{1}H NMR (DMSO-d_6, 600 MHz): δ 11.04 (s, 1H), 10.97 (s, 1H), 10.83 (s, 1H), 8.39 (s, 1H), 8.05 (s, 1H), 7.84 (d, J = 7.9 Hz, 1H), 7.81 (s, 1H), 7.67 (d, J = 8.5 Hz, 1H), 7.65 (d, J = 8.5 Hz, 1H), 7.48 (s, 1H), 7.43 (s, 1H), 7.41 (d, J = 15.5 Hz, 1H), 7.34 (d, J = 7.6 Hz, 1H), 6.41 (d, J = 15.8 Hz, 1H), 3.92 (s, 3H), 1.21 (s, 1H). HRMS calcd for $C_{21}H_{19}N_4O_6$ 423.1642 $(M+H)^+$, found 423.1645.

4.3. Biological evaluation

4.3.1. IMPDH inhibition

IMPDH inhibition assays were performed as previously described.[38] Briefly, assays were set up in duplicate using IMPDH type 1 (150 nM) and type 2 (50 nM) and varying concentrations of

inhibitor. IMPDH and inhibitors were added to 100 μL reaction buffer (50 mM Tris, pH 8.0, 100 mM KCl, 1 mM DTT, 100 μM IMP, 100 μM NAD) at 25 °C, mixed gently and the production of NADH was monitored by following changes in absorbance at 340 nm on a Molecular Devices M5e multimode plate reader. Steady state velocities were used to determine IC50 and K_i^{app} values by fitting the velocities versus inhibitor concentration to the sigmoidal concentration-response curve (variable slope) and the Morrison equation,[39] respectively, using GraphPad Prism.

4.3.2. HDAC inhibition

HDAC inhibition assays were performed using the HDAC Activity/Inhibitor Screening Assay Kit (Cayman Chemical) per the manufacturer's instructions. Inhibitors were suspended in either DMSO or methanol. End point readings were used to determine IC_{50} values by fitting the fractional fluorescence versus inhibitor concentration to the sigmoidal concentration-response curve (variable slope) using GraphPad Prism. Curves were corrected for Auto-fluorescence by making a standard concentration curve, substituting compound for solvent using the background well conditions.

4.3.3. Inhibition of proliferation of K562 cells

About 2000 cells/well of logarithmically growing human myelogenous leukemia K562 cells were plated into 96-well plates and incubated at 37 °C for 24 h. Compounds at final concentrations up to 100 μM was added in duplicate wells in 0.15% DMSO (final concentration), mixed and incubated for 72 h. At the end of the incubation period, 20 μL of MTS reagent was added, mixed and further incubated for 3 h and then absorbance was read at 490 nm in a plate reader. Control cells exhibited 3-doublings (doubling time was 24 h).

4.4. Computational modeling

All modeling was carried out using the Schrodinger modeling package.[40] The structure of HDAC1 was homology modeled based on the solved X-ray crystallographic structure of histone deacetylase-like protein (HDLP) in complex with SAHA (PDB: 1C3S).[37] The initial sequence alignment of HDAC1-11 and HDLP using clustalW showed HDAC2-3, 8 and HDLP have the highest sequence similarity to HDAC1 with 59% sequence identity for the SAHA binding site (see Supplementary Fig. S1). The homology model of HDAC1 was then carried out based on the structure conserved regions identified by multiple sequence alignment of HDAC1-3, 8 and HLDP (see Supplementary Fig. S2). SAHA and compound **16a** were docked[41] into the HDAC1 binding site based on predefined constraints of H141, Y303 and zinc ion. Modeling of compound **18a** and **18b** into the NAD binding pocket of the solved X-ray crystallographic structure of *h*IMPDH2 (PDB: 1NF7) was based on the previously reported mode of binding of Vertex compound VX-497 in H93A *Cricetulus griseus* IMPDH.[14] Distance restraints between oxazolyl group and G326 and T333 was used during minimization to reproduce the observe hydrogen bonding observed in X-ray crystallographic studies. To account for solvent effect and protein flexibility, each of the modeled complexes was further refined by restraint energy minimization using OPLSAA 2005 forcefield[42] within 20 Å TIP3P[43] surface constrained water sphere. To identify key amino residues involved in the ligand binding, the non-bond per residue interaction energies between each modeled ligand and individual amino acid residues within the binding site were evaluated with a dielectric constant of 4.

Acknowledgments

This research was supported by the Center for Drug Design in the Academic Health Center of the University of Minnesota. We thank Dr. Courtney Aldrich for his help with the biological assays. We also thank Dr. Yanli Xu for her help with HRMS characterization of several compounds. The University of Minnesota Supercomputing Institute provided all the computational resources.

Supplementary data

Supplementary data associated with this article can be found, in the online version, at doi:10.1016/j.bmc.2010.06.081.

References and notes

1. Hanahan, D.; Weinberg, R. A. *Cell* **2000**, *100*, 57–70.
2. Daub, H.; Specht, K.; Ullrich, A. *Nat. Rev. Drug Disc.* **2004**, *3*, 1001–1010.
3. Soverini, S.; Iacobucci, I.; Baccarani, M.; Martinelli, G. *Haematologica* **2007**, *92*, 437–439.
4. Quintas-Cardama, A.; Cortes, J. *Blood* **2009**, *113*, 1619–1630.
5. Walz, C.; Sattler, M. *Crit. Rev. Oncol. Hematol.* **2006**, *57*, 145–164.
6. Martinelli, G.; Soverini, S.; Rosti, G.; Baccarani, M. *Leukemia* **2005**, *19*, 1872–1879.
7. Johnstone, R. W. *Nat. Rev. Drug Disc.* **2002**, *1*, 287–299.
8. Johnstone, R. W.; Licht, J. D. *Cancer Cell* **2003**, *4*, 13–18.
9. Bolden, J. E.; Peart, M. J.; Johnstone, R. W. *Nat. Rev. Drug Disc.* **2006**, *5*, 769–784.
10. Hedstrom, L. *Chem. Rev.* **2009**, *109*, 2903–2928.
11. Chen, L.; Pankiewicz, K. W. *Curr. Opin. Drug Discov. Devel.* **2007**, *10*, 403–412.
12. Chen, L.; Petrelli, R.; Felczak, K.; Gao, G.; Bonnac, L.; Yu, J. S.; Bennett, E. M.; Pankiewicz, K. W. *Curr. Med. Chem.* **2008**, *15*, 650–670.
13. Miller, T. A.; Witter, D. J.; Belvedere, S. *J. Med. Chem.* **2003**, *46*, 5097–5116.
14. Sintchak, M. D.; Nimmesgern, E. *Immunopharmacology* **2000**, *47*, 163–184.
15. Jain, J.; Almquist, S. J.; Heiser, A. D.; Shlyakhter, D.; Leon, E.; Memmott, C.; Moody, C. S.; Nimmesgern, E.; Decker, C. *J. Pharmacol. Exp. Ther.* **2002**, *302*, 1272–1277.
16. Dhar, T. G. M.; Shen, Z. Q.; Fleener, C. A.; Rouleau, K. A.; Barrish, J. C.; Hollenbaugh, D. L.; Iwanowicz, E. J. *Bioorg. Med. Chem. Lett.* **2002**, *12*, 3305–3308.
17. Dhar, T. G. M.; Shen, Z. Q.; Gu, H. H.; Chen, P.; Norris, D.; Watterson, S. H.; Ballentine, S. K.; Fleener, C. A.; Rouleau, K. A.; Barrish, J. C.; Townsend, R.; Hollenbaugh, D. L.; Iwanowicz, E. J. *Bioorg. Med. Chem. Lett.* **2003**, *13*, 3557–3560.
18. Chen, P.; Norris, D.; Haslow, K. D.; Dhar, T. G. M.; Pitts, W. J.; Watterson, S. H.; Cheney, D. L.; Bassolino, D. A.; Fleener, C. A.; Rouleau, K. A.; Hollenbaugh, D. L.; Townsend, R. M.; Barrish, J. C.; Iwanowicz, E. J. *Bioorg. Med. Chem. Lett.* **2003**, *13*, 1345–1348.
19. Watterson, S. H.; Chen, P.; Zhao, Y.; Gu, H. H.; Dhar, T. G.; Xiao, Z.; Ballentine, S. K.; Shen, Z.; Fleener, C. A.; Rouleau, K. A.; Obermeier, M.; Yang, Z.; McIntyre, K. W.; Shuster, D. J.; Witmer, M.; Dambach, D.; Chao, S.; Mathur, A.; Chen, B. C.; Barrish, J. C.; Robl, J. A.; Townsend, R.; Iwanowicz, E. J. *J. Med. Chem.* **2007**, *50*, 3730–3742.
20. Watterson, S. H.; Liu, C. J.; Dhar, T. G. M.; Gu, H. H.; Pitts, W. J.; Barrish, J. C.; Fleener, C. A.; Rouleau, K.; Sherbina, N. Z.; Hollenbaugh, D. L.; Iwanowicz, E. J. *Bioorg. Med. Chem. Lett.* **2002**, *12*, 2879–2882.
21. Gu, H. H.; Iwanowicz, E. J.; Guo, J. Q.; Watterson, S. H.; Shen, Z. Q.; Pitts, W. J.; Dhar, T. G. M.; Fleener, C. A.; Rouleau, K.; Sherbina, N. Z.; Witmer, M.; Tredup, J.; Hollenbaugh, D. *Bioorg. Med. Chem. Lett.* **2002**, *12*, 1323–1326.
22. Iwanowicz, E. J.; Watterson, S. H.; Liu, C. J.; Gu, H. H.; Mitt, T.; Leftheris, K.; Barrish, J. C.; Fleener, C. A.; Rouleau, K.; Sherbina, N. Z.; Hollenbaugh, D. L. *Bioorg. Med. Chem. Lett.* **2002**, *12*, 2931–2934.
23. Pitts, W. J.; Guo, J. Q.; Dhar, T. G. M.; Shen, Z. Q.; Gu, H. H.; Watterson, S. H.; Bednarz, M. S.; Chen, B. C.; Barrish, J. C.; Bassolino, D.; Cheney, D.; Fleener, C. A.; Rouleau, K. A.; Hollenbaugh, D. L.; Iwanowicz, E. J. *Bioorg. Med. Chem. Lett.* **2002**, *12*, 2137–2140.
24. Iwanowicz, E. J.; Watterson, S. H.; Guo, J. Q.; Pitts, W. J.; Dhar, T. G. M.; Shen, Z. Q.; Chen, P.; Gu, H. H.; Fleener, C. A.; Rouleau, K. A.; Cheney, D. L.; Townsend, R. M.; Hollenbaugh, D. L. *Bioorg. Med. Chem. Lett.* **2003**, *13*, 2059–2063.
25. Dhar, T. G. M.; Shen, Z. Q.; Guo, J. Q.; Liu, C. J.; Watterson, S. H.; Gu, H. H.; Pitts, W. J.; Fleener, C. A.; Rouleau, K. A.; Sherbina, N. Z.; McIntyre, K. W.; Shuster, D. J.; Witmer, M. R.; Tredup, J. A.; Chen, B. C.; Zhao, R. L.; Bednarz, M. S.; Cheney, D. L.; MacMaster, J. F.; Miller, L. M.; Berry, K. K.; Harper, T. W.; Barrish, J. C.; Hollenbaugh, D. L.; Iwanowicz, E. J. *J. Med. Chem.* **2002**, *45*, 2127–2130.
26. Watterson, S. H.; Carlsen, M.; Dhar, T. G. M.; Shen, Z. Q.; Pitts, W. J.; Guo, J. Q.; Gu, H. H.; Norris, D.; Chorba, J.; Chen, P.; Cheney, D.; Witmer, M.; Fleener, C. A.; Rouleau, K.; Townsend, R.; Hollenbaugh, D. L.; Iwanowicz, E. J. *Bioorg. Med. Chem. Lett.* **2003**, *13*, 543–546.
27. Watterson, S. H.; Dhar, T. G. M.; Ballentine, S. K.; Shen, Z. Q.; Barrish, J. C.; Cheney, D.; Fleener, C. A.; Rouleau, K. A.; Townsend, R.; Hollenbaugh, D. L.; Iwanowicz, E. J. *Bioorg. Med. Chem. Lett.* **2003**, *13*, 1273–1276.
28. Buckley, G. M.; Davies, N.; Dyke, H. J.; Gilbert, P. J.; Hannah, D. R.; Haughan, A. F.; Hunt, C. A.; Pitt, W. R.; Profit, R. H.; Ray, N. C.; Richard, M. D.; Sharpe, A.; Taylor, A. J.; Whitworth, J. M.; Williams, S. C. *Bioorg. Med. Chem. Lett.* **2005**, *15*, 751–754.
29. Chen, L.; Wilson, D.; Jayaram, H. N.; Pankiewicz, K. W. *J. Med. Chem.* **2007**, *50*, 6685–6691.

30. Mahboobi, S.; Dove, S.; Sellmer, A.; Winkler, M.; Eichhorn, E.; Pongratz, H.; Ciossek, T.; Baer, T.; Maier, T.; Beckers, T. *J. Med. Chem.* **2009**, *52*, 2265–2279.
31. Cai, X.; Zhai, H. X.; Wang, J.; Forrester, J.; Qu, H.; Yin, L.; Lai, C. J.; Bao, R.; Qian, C. *J. Med. Chem.* **2010**, *53*, 2000–2009.
32. Yen, S. K.; Koh, L. L.; Hahn, F. E.; Huynh, H. V.; Hor, T. S. A. *Organometallics* **2006**, *25*, 5105–5112.
33. Niiya, K.; Thompson, R. D.; Silvia, S. K.; Olsson, R. A. *J. Med. Chem.* **1992**, *35*, 4562–4566.
34. Mackman, R. L.; Katz, B. A.; Breitenbucher, J. G.; Hui, H. C.; Verner, E.; Luong, C.; Liu, L.; Sprengeler, P. A. *J. Med. Chem.* **2001**, *44*, 3856–3871.
35. Jain, J.; Almquist, S. J.; Shlyakhter, D.; Harding, M. W. *J. Pharm. Sci.* **2001**, *90*, 625–637.
36. Remiszewski, S. W.; Sambucetti, L. C.; Bair, K. W.; Bontempo, J.; Cesarz, D.; Chandramouli, N.; Chen, R.; Cheung, M.; Cornell-Kennon, S.; Dean, K.; Diamantidis, G.; France, D.; Green, M. A.; Howell, K. L.; Kashi, R.; Kwon, P.; Lassota, P.; Martin, M. S.; Mou, Y.; Perez, L. B.; Sharma, S.; Smith, T.; Sorensen, E.; Taplin, F.; Trogani, N.; Versace, R.; Walker, H.; Weltchek-Engler, S.; Wood, A.; Wu, A.; Atadja, P. *J. Med. Chem.* **2003**, *46*, 4609–4624.
37. Finnin, M. S.; Donigian, J. R.; Cohen, A.; Richon, V. M.; Rifkind, R. A.; Marks, P. A.; Breslow, R.; Pavletich, N. P. *Nature* **1999**, *401*, 188–193.
38. Umejiego, N. N.; Li, C.; Riera, T.; Hedstrom, L.; Striepen, B. *J. Biol. Chem.* **2004**, *279*, 40320–40327.
39. Morrison, J. F. *Biochim. Biophys. Acta* **1969**, *185*, 269–286.
40. Maestro v9.0, Glide v5.5, Prime v2.1, Macromodel v9.7, Schrodinger, LLC, New York, NY, 2009.
41. Friesner, R. A.; Murphy, R. B.; Repasky, M. P.; Frye, L. L.; Greenwood, J. R.; Halgren, T. A.; Sanschagrin, P. C.; Mainz, D. T. *J. Med. Chem.* **2006**, *49*, 6177–6196.
42. Jorgensen, W. L.; Maxwell, D. S.; TiradoRives, J. *J. Am. Chem. Soc.* **1996**, *118*, 11225–11236.
43. Jorgensen, W. L.; Chandrasekhar, J.; Madura, J. D.; Impey, R. W.; Klein, M. L. *J. Chem. Phys.* **1983**, *79*, 926–935.